Impacts of metal mining on river systems: a global assessment

Macklin, M.G.; Thomas, Christopher; Mudbhatkal, Amogh; Brewer, P.A.; Hudson-Edwards, Karen; Lewin, John; Scussolini, Paul; D. Eilander, Dirk; Lechner, Alex; Owen, John; Bird, Graham; Kemp, Deanna; Mangalaa, K

Science

DOI:
10.1126/science.adg670

Published: 22/09/2023

Peer reviewed version

Title: Impacts of metal mining on river systems: a global assessment

Authors: M.G. Macklin[1,2,3*], C.J. Thomas[1,4], A. Mudbhatkal[1], P.A. Brewer[5], K.A. Hudson-Edwards[6], J. Lewin[5], P. Scussolini[7], D. Eilander[7,8], A. Lechner[9], J. Owen[10], G. Bird[11], D. Kemp[12], K. R. Mangalaa[13]

Affiliations:

[1] Lincoln Centre for Water and Planetary Health, University of Lincoln; Lincoln, UK.

[2] Innovative River Solutions, Institute of Agriculture and Environment, Massey University; New Zealand.

[3] Centre for the Study of the Inland, La Trobe University; Melbourne, Australia.

[4] University of Namibia, Windhoek; Namibia.

[5] Department of Geography and Earth Sciences, Aberystwyth University; Aberystwyth, Ceredigion, UK.

[6] Environment & Sustainability Institute and Camborne School of Mines, University of Exeter; Penryn, Cornwall, UK.

[7] Institute for Environmental Studies, Vrije Universiteit Amsterdam; Amsterdam, Netherlands.

[8] Department of Inland Water Systems, Deltares, Delft, The Netherlands Institute for Environmental Studies, Vrije Universiteit Amsterdam, Amsterdam, Netherlands.

[9] Monash University Indonesia; Jakarta, Indonesia.

[10] Centre for Development Support, University of the Free State; South Africa.

[11] School of Natural Sciences, Bangor University; Bangor, Gwynedd, UK.

[12] Centre for Social Responsibility in Mining, Sustainable Minerals Institute, The University of Queensland; St Lucia, Australia.

[13] Ministry of Earth Sciences, Government of India, New Delhi, India.

*Corresponding author. Email: mmacklin@lincoln.ac.uk

Abstract:

An estimated 23 M people live on floodplains affected by potentially dangerous concentrations of toxic waste derived from past and present metal mining activity. We analyze the global dimensions of this hazard, particularly Pb, Zn, Cu and As, using a geo-referenced global database detailing all known metal mining sites, and intact/failed tailings storage facilities. We then use process-based and empirically tested modelling, to produce a global assessment of metal mining contamination in river systems, and the number of human populations, and livestock exposed. Worldwide, metal mines impact 479,200 km of river channels and 164,000 km^2 of floodplains. The number of people exposed to contamination sourced from long-term discharge

of mining waste into rivers is almost fifty times greater than the number directly impacted by tailings dam failures.

One-Sentence Summary: High levels of river and floodplain metal contamination are revealed across the globe from active and inactive metal mining sites.

Metal Mining and the River Environment

In 2018, mining had a market capital value of almost a trillion US dollars, and $600 billion in revenue *(1)*. It has been estimated that the annual production of solid mine wastes (including those from metal mining) now makes up one third of the sediment budget for the Earth (*2, 3*), and that ~1 million km^2 of the World is covered with mine waste *(4)*. Many of the richest geological deposits are being or have already been exploited, and companies are now turning to deposits with lower-grade ores. These lower grade ores generate more waste per unit extracted and damage to the Earth's surface is likely to be exacerbated (*5*). Some of these wastes contain elements, such as arsenic, lead and mercury, in concentrations that may pose a serious hazard, and potential risk, to ecosystem and human health at multiple trophic levels (*6*).

Various multi-link exposure pathways exist for humans to ingest or inhale contaminant metals from mine sites and floodplain soils (*6*). For example, plants and crops grown domestically or commercially on contaminated soils, or irrigated by water contaminated by mine waste, frequently contain high concentrations of metals and metalloids (hereafter referred to as 'metals') *(7-9)*. Animals grazing on floodplains may then eat this plant material and sediment, especially after flooding, when fresh metal-rich sediment is deposited *(10)*. This poses a potential risk to their health and that of humans who consume their meat and milk (*10, 11*). Fish and shellfish are also significant accumulators of metals and represent an important route by which contaminants enter the food chain, especially in communities that rely on aquatic resources (*12, 13*). In tropical and sub-tropical regions, the consumption of insects (entomophagy) is becoming an increasingly important source of protein, especially where human populations do not have access to meat. Metals bioaccumulate in insects that live in close proximity to mine sites, which can then pose a potential health risk to humans who use entomophagy as a major protein source (*14*).

Metal mining represents humankind's earliest and most persistent form of environmental contamination. Waste from mining began to contaminate river systems as early as 7,000 years ago *(15)*. Water was usually involved in extraction and processing of metal ores, resulting in metals (both dissolved and sediment-associated) being supplied to streams and rivers, dispersed downstream, and then deposited across floodplains that were used for agricultural food production. Since the mid-nineteenth century, tailings dams have been used to store mine waste, which has reduced direct supply into rivers. However, such structures are prone to failure with often severe consequences for ecosystems and human communities downstream *(16)*.

Path-making research (*17-19*) over the last 40 years has demonstrated the role of dispersal *(20)*, storage *(21-23)* and remobilization *(24)* processes in the environmental fate of metals within rivers affected by metal mining, including those impacted by long term mining activities as well as those contaminated by tailings dam failures (TDFs). These studies have shown that more than 90% of metals are sediment associated, are transported 10-100 km downstream from the point where mining operations discharge into a watercourse, and are deposited and stored along river channels and especially on floodplains for extended (10^2-10^4 years) time periods *(18, 25)*. In the first industrial nations of Western Europe, and the USA, flood-related remobilization of contaminated floodplain sediment, resulting from historical mining during the 19th and early 20th century *(19, 21, 24)*, now constitutes the primary source of metal contaminants in rivers. Small catchments (<500 km^2) can be extremely contaminated, but the larger rivers into which they feed tend to have significantly lower contamination levels because metal mine waste is either stored in upstream floodplains (*26*), or is diluted by uncontaminated sediment from non-mining sources *(27)*.

Here we bring together all spatial data that can at present be obtained globally on metal mines (both active and inactive) and tailings dams, including those that have failed. We then calculate the area of floodplains, and the number of people and livestock potentially exposed (see SI Materials and Methods (*28*)). This quantifies, for the first time, the off-site environmental impacts of metal mining activity on river systems worldwide, and the consequent number of people/livestock that could potentially be exposed to unacceptably high concentrations of toxic metals.

Methodology:

Data on active (defined as still in operation in database sources published/accessed before August 29th 2022) and inactive (defined in database sources as closed) metal mines worldwide, including their location, mineral commodities, and operational status, were compiled into the Water and Planetary Health Analytics (WAPHA) global metal mines database (*29*) using QGIS (*30*). Mine information was acquired from the United States Geological Survey Mineral Resources Data System (*31*) (73,917 mines worldwide), the BritPits database of the British Geological Survey (*32*) (8,459 mines in the United Kingdom), the S&P Global Market Intelligence database (*33*) (2,584 mines worldwide), and our own compilation of c. 100,000 additional mines from academic and gray literature, including regional data published by government agencies and industry (tables S1-S2). Twenty-one types of active and inactive metal mines were used in our modelling and analysis (tables S3a-S3b). We also compiled a georeferenced global database of metal mining tailings storage facilities and tailings dam failures based on the ICOLD/UNEP 2001 compilation (Bulletin 121) (*34*), the World Information Service on Energy (*35*), the World Mine Tailings Failures and Global Tailings Portal databases (*36*), in conjunction with our own compilation of source literature published by government and non-government organizations (*29*) (tables S4-S5).Together these spatial data represent, to our knowledge, the most comprehensive compilation of metal mine locations to date.

We identified catchments affected by active and inactive metal mining by overlaying in MATLAB (*37*) all mines, tailings storage facilities and tailings dam failures onto level 4 polygons of the HydroBASINS modelling framework (*38*). These depict watershed boundaries and sub-basin delineations at 15 arc second resolution. Within all sub-basins we estimated the length of river channel (km), the floodplain area (km^2) and the 100-year flood inundation area (km^2) downstream of each mine likely to be contaminated, by using a new process-based model of sediment-associated mining contaminant dispersal (figs S1-S12, table S6). This model calculates the extent downstream of a mine where concentrations of metal (Cu c.10.3 km; Pb c. 8.6 km; Zn c. 6.5 km) and As (c. 45.6 km) in river channel and floodplain sediments exceed guideline values for intervention and remediation (table S7). We ground-truthed our results in fifteen catchments across Europe (UK, Romania, Bulgaria), ranging in size from 46 to 232,193 km^2 (tables S8-S11). Where tailings dams have failed and their pre-failure crest-height and volume of impounded waste are known (165 from a total of 257), the length of river channel and area of floodplain affected was calculated (*39*). Using the Socioeconomic Data and Applications Center (NASA-SEDAC) population data of the year 2020 (*40*), and FAO Gridded Livestock of the World database (GLW v3.1) (*41*), the number of people and livestock (cattle, goat, and sheep) living on mining-affected floodplains was determined (tables S12-S14). The area of irrigated land based on FAO Global Map of Irrigation Areas (GMIA) in mining-impacted floodplains was also calculated (table S15). Our geospatial integration of metal mine, tailings storage facilities, tailings dam failures, hydrographic, geomorphic, demographic and livestock databases enable us to evaluate globally the human population directly exposed and the number of livestock in contaminated areas with the potential for uptake of contaminant metals into the human food chain (table S15).

Results:

Worldwide there are recorded 22,609 active and 159,735 abandoned mines, 11,587 tailings storage facilities and a further 257 reported tailings dam failures (Fig 1). Metal mining has affected some 164,400 km^2 of floodplains (112,400 km^2 from inactive mines; 52,000 km^2 from active mines) and 480,700 km of river channels (inactive, 365,200 km; active, 114,000 km) are affected by mining (Fig. 2; table S16). We estimate that 23.48 M people live on mining-affected floodplains that also support 5.72 M livestock and include 65,600 km^2 of irrigated land (Fig 3; table S16). Disaggregated on a continental scale, North America (active 11,871; inactive 80,995) and Oceania (active 3,430; inactive 53,233) have the largest number of mines followed by South America (active 3,240; inactive 14,577), Europe (active 1,024; inactive 9,080), Asia (active 1,817; inactive 1,473), and Africa (active 1,227; inactive 377) (table S1). Oceania, Europe, North America, and South America are mostly affected by inactive mining, while active mining activities are more important in Africa and Asia (table S1).

North America stands out as the most impacted region in terms of river length (198,400 km) and surface area of floodplains (43,100 km^2) (Fig 3; table S16). River channels and floodplains are also significantly impacted in Oceania (river length 106,100 km; floodplain 33,800 km^2), South America (81,700 km; 38,600 km^2) and Asia (60,900 km; 33,500 km^2), but to a lesser extent in Europe (14,800 km; 4,900 km^2) and Africa (17,300 km; 10,400 km^2) (Fig 3; table S16). Asia, with 14.53 M people living in affected floodplains is the most vulnerable region in terms of human exposure, followed by North America (4.09 M), Europe (1.73 M), South America (1.53 M), Africa (1.19 M) and Oceania (0.42 M) (Fig 3; table S16).

Undertaking the same audit for river catchments in which tailings dams have failed is less straightforward because data on dam height and volume of waste stored is only available for 165 of 257 recorded failures. Worldwide we calculate, using this large but incomplete database, that a minimum of 5,300 km of river channels and 4,950 km^2 of floodplains have been affected by TDFs (Fig 3; table S17). The number of people living on floodplains that have been directly affected by TDFs is substantial (0.32 M) (Fig 3; table S17), but our modelling indicates that the impact of these events on river systems, and potential human population / livestock exposure, is two or three orders of magnitude smaller than in basins that have experienced inactive and/or active mining activity (Fig 3; table S17). This reflects the small count of TDFs compared to the much larger number of active and inactive mines worldwide.

Gauged by the number of people living on floodplains affected by mining activity, populations in China (9.74 M) and the USA (3.17 M) are potentially most at risk of exposure to contaminant metals and metalloids (tables S12-S14). Surprisingly, South Korea (0.79 M), Germany (0.35 M) and the UK (0.31 M) are ranked globally in the top 12 (table S13) in terms of population exposed to riverine related metal hazards, with the environmental legacy of historical mining being most problematic in Western Europe. Countries that by world standards have relatively short rivers (e.g., Chile, Japan, New Zealand, South Korea, UK), and particularly those with low sediment loads (e.g., Germany, UK), have higher levels of river channel and floodplain contamination (table S15) as a consequence of limited dilution of sediment-associated mine waste *(42)*.

Implications for Ecosystem and Human Health:

This global survey of the environmental impacts of metal mining, and the consequent potential exposure risk of humans and livestock to toxic metals, reveals that an estimated 23 M people live on floodplains affected by potentially hazardous concentrations of toxic waste derived from historical and/or active upstream mining activity. However, because of incomplete reporting of mine locations and tailings dam failures, most notably within China, India, and Russia, this is certainly an underestimation of the population at risk. In addition, the impacts of modern artisanal mining on river systems in the global south are still very poorly documented, and this should be the next critical step for understanding the worldwide impact of mining.

Ecological and societal impacts of recent tailings dam failures are locally catastrophic and have resulted in significant loss of life (*5*). However, our assessment indicates that the number of people likely to be exposed to unacceptably high concentrations of toxic metals by these accidents (estimated to be more than 0.32 M) is almost fifty times smaller than in river floodplains affected by historical (11.39 M) and active (12.08 M) metal mining. Exposure of workers directly engaged in current industrial metal mining and ore processing, smelting and small-scale artisanal mining, which are three of the top five polluting industries worldwide (*43*), are not captured by our study. Preliminary modeling suggests that these industries pose a risk to health of between 18 to 23 M people (*43*), which is comparable to the number of people we have estimated that live on mining contaminated floodplains worldwide (table S16). Our georeferenced database and process-based predictive modelling provide tools for locating areas of highest potential exposure where monitoring, and potentially intervention, should be prioritized (see tables S12-S14), and further highlights catchments (see figs S9-12) where new data are required. These would include locations in the historically mined regions of Andean South America, Australia (Victoria), Southeast and Central Asia (Pamir and Tien Shan), North America, and the UK (Wales and northern England; Fig 4), in addition to those in Amazonia, Sub-Saharan Africa, Southeast Asia, southern and eastern China where most of the world's new but poorly regulated mining operations are located (table S13).

We conclude that metal mining contamination of rivers and floodplains poses a possible significant additional hazard to the health of both urban and rural communities in Africa and Asia that are already burdened with water-related diseases. For the first industrial nations of Western Europe and the USA, this contamination constitutes a major and growing constraint to water and food security, compromises ecosystem services *(44)*, and increases antimicrobial resistance in the environment (*45*). But global, multi-scalar, data with sufficient granularity are not presently available to quantify potential risks to ecosystem and human health. For example, the export of food produced on contaminated floodplains will often enter a spatially extensive food chain, and this will require new human biomonitoring and food basket studies (*46*). However, existing evidence already demonstrates that human health can be directly affected through the ingestion, inhalation and absorption of metal contaminated soil, and indirectly through the quantity and quality of food that is derived from soil-based agriculture (*9, 14, 47-49*).

Increasing frequency of river flooding associated with anthropogenic global climate warming *(50)* can result in augmented erosion and sediment-associated metal remobilization from recently and historically contaminated floodplains (*10, 24, 51*), that now in many parts of the world constitute the principal source of metal contaminants in rivers. In addition, because of rapid urbanization and increasing settlement in floodplains worldwide (notably in Sub-Saharan Africa and South Asia), the proportion of population exposed to flooding and contaminated flood waters has risen by 20-24% from 2000-2025 (*52*). Expansion of lower grade metal ore mining, which generates more waste per unit extracted, coupled with an increasing frequency of catastrophic tailings dam failures (*53*), underlines the need to routinely incorporate outputs from large-scale mining databases (as reported here) into environmental monitoring programs and metal exposure pathway analyses. This will facilitate better management of metal contamination and risk of exposure downstream of historically and active metal mine sites.

Reference List

1. PWC, "Mine 2018: Tempting Times", (2018) https://www.pwc.com/id/en/publications/assets/eumpublications/mining/mine-2018.pdf.
2. U. Förstner, "Introduction" in *Environmental Impacts of Mining Activities: Emphasis on Mitigation and Remedial Measures,* J. M. Azcue, Ed. (Springer, 1999), pp. 1-3.
3. J. Syvitski *et al.*, Earth's sediment cycle during the Anthropocene. *Nature Reviews Earth and Environment* **3**, 179-196 (2022).
4. B. G. Lottermoser, *Mine Wastes: Characterization, Treatment and Environmental Impacts* (Springer, ed. 3, 2010).
5. K. A. Hudson-Edwards, Tackling mine wastes. *Science* **352**, 288-290 (2016).
6. J. E. Gall *et al.*, Transfer of heavy metals through terrestrial food webs: a review. *Environ Monit Assess* **187**, 201 (2015).
7. J. R. Miller *et al.*, Heavy metal contamination of water, soil and produce within riverine communities of the Rio Pilcomayo basin, Bolivia. *Sci Total Environ* **320**, 189-209 (2004).
8. D. Xu *et al.*, Effects of soil properties on heavy metal bioavailability and accumulation in crop grains under different farmland use patterns. *Sci Rep-Uk* **12**, 9211 (2022).
9. M. Roy, L. M. McDonald, Metal Uptake in Plants and Health Risk Assessments in Metal-Contaminated Smelter Soils. *Land Degradation & Development* **26**, 785-792 (2015).
10. S. A. Foulds *et al.*, Flood-related contamination in catchments affected by historical metal mining: An unexpected and emerging hazard of climate change. *Sci Total Environ* **476**, 165-180 (2014).
11. S. Giri, A. K. Singh, Human health risk assessment due to metals in cow's milk from Singhbhum copper and iron mining areas, India. *J Food Sci Technol* **57**, 1415-1420 (2020).
12. H. Ali, E. Khan, Bioaccumulation of non-essential hazardous heavy metals and metalloids in freshwater fish. Risk to human health. *Environmental Chemistry Letters* **16**, 903-917 (2018).
13. Y. Jia *et al.*, Distribution, contamination and accumulation of heavy metals in water, sediments, and freshwater shellfish from Liuyang River, Southern China. *Environ Sci Pollut R* **25**, 7012-7020 (2018).
14. S. Mwelwa *et al.*, Biotransfer of heavy metals along the soil-plant-edible insect-human food chain in Africa. *Sci Total Environ* **881**, 163150 (2023).
15. J. P. Grattan *et al.*, The first polluted river? Repeated copper contamination of fluvial sediments associated with Late Neolithic human activity in southern Jordan. *Sci Total Environ* **573**, 247-257 (2016).
16. D. Kossoff *et al.*, Mine tailings dams: Characteristics, failure, environmental impacts, and remediation. *Appl Geochem* **51**, 229-245 (2014).
17. J. Lewin *et al.*, "Interactions Between Channel Change and Historic Mining Sediments" in *River Channel Changes*, K. J. Gregory, Ed. (John Wiley and Sons, 1977), pp. 353-367.
18. J. Lewin, M. G. Macklin, "Metal mining and floodplain sedimentation in Britain" in *International Geomorphology Part 1,* V. Gardiner, Ed. (John Wiley and Sons, 1987), pp. 1009-1027.
19. W. L. Graf *et al.*, Geomorphology of Heavy-Metals in the Sediments of Queen-Creek, Arizona, USA. *Catena* **18**, 567-582 (1991).

20. M. G. Macklin, J. Lewin, Sediment Transfer and Transformation of an Alluvial Valley Floor - the River South Tyne, Northumbria, UK. *Earth Surf Proc Land* **14**, 233-246 (1989).
21. M. G. Macklin, R. B. Dowsett, The Chemical and Physical Speciation of Trace-Metals in Fine-Grained Overbank Flood Sediments in the Tyne Basin, Northeast England. *Catena* **16**, 135-151 (1989).
22. M. G. Macklin *et al.*, The significance of pollution from historic metal mining in the Pennine orefields on river sediment contaminant fluxes to the North Sea. *Sci Total Environ* **194**, 391-397 (1997).
23. J. M. Martin, M. Meybeck, Elemental Mass-Balance of Material Carried by Major World Rivers. *Mar Chem* **7**, 173-206 (1979).
24. I. A. Dennis *et al.*, The impact of the October-November 2000 floods on contaminant metal dispersal in the River Swale catchment, North Yorkshire, UK. *Hydrol Process* **17**, 1641-1657 (2003).
25. M. G. Macklin *et al.*, A geomorphological approach to the management of rivers contaminated by metal mining. *Geomorphology* **79**, 423-447 (2006).
26. I. A. Dennis *et al.*, The role of floodplains in attenuating contaminated sediment fluxes in formerly mined drainage basins. *Earth Surf Proc Land* **34**, 453-466 (2009).
27. D. Ciszewski, T. M. Grygar, A Review of Flood-Related Storage and Remobilization of Heavy Metal Pollutants in River Systems. *Water Air Soil Poll* **227**, (2016).
28. M. G. Macklin *et al.*, Materials and Methods for: Impacts of metal mining on river systems: a global assessment. (Supplementary Information, 2023).
29. "Water and Planetary Health Analytics (WAPHA) Global Metal Mines Database", (2023);
30. QGIS Association, "QGIS Geographic Information System", (2023); http://www.qgis.org/.
31. USGS, "Mineral Resources Data System (MRDS)", (2022); https://mrdata.usgs.gov/mrds/.
32. BGS, "User Guide: BGS BritPIts", (2021); https://www.bgs.ac.uk/datasets/britpits/.
33. S&P Global Market Intelligence, "S&P Capital IQ Pro platform", https://www.spglobal.com/marketintelligence/en/campaigns/metals-mining.
34. ICOLD, *Tailings Dams: Risk of Dangerous Occurrences : Lessons Learnt from Practical Experiences (bulletin 121)*. (Commission Internationale des Grand Barrages, 2001).
35. WISE Uranium Project, "Chronology of major tailings dam failures (1960-2022)", (2022); https://wise-uranium.org/mdaf.html.
36. GTP, "Global Tailings Portal", https://tailing.grida.no/.
37. "MATLAB version: 9.9.0 (R2020b), Natick, Massachusetts: The MathWorks Inc", (2020); https://www.mathworks.com.
38. HydroSheds, "Seamless hydrographic data for global and regional applications v1", https://www.hydrosheds.org/.
39. P. Concha Larrauri, U. Lall, Tailings Dams Failures: Updated Statistical Model for Discharge Volume and Runout. *Environments* **5**, (2018).
40. NASA, "Gridded Population of the World (GPW), v4 rev 10", (2016); https://sedac.ciesin.columbia.edu/data/collection/gpw-v4/whatsnewrev10.
41. FAO, "Gridded Livestock of the World (GLW3)", (2010); https://www.fao.org/land-water/land/land-governance/land-resources-planning-toolbox/category/details/fr/c/1236449/.

42. G. Bird *et al.*, Dispersal of Contaminant Metals in the Mining-Affected Danube and Maritsa Drainage Basins, Bulgaria, Eastern Europe. *Water Air Soil Poll* **206**, 105-127 (2010).
43. P. E. a. G. C. Switzerland, "World's Worst Pollution Problems: The Toxins Beneath Our Feet", (2016) http://www.worstpolluted.org/2016-report.html.
44. K. B. Ding *et al.*, Ecosystem services provided by heavy metal-contaminated soils in China. *J Soil Sediment* **18**, 380-390 (2018).
45. C. Baker-Austin *et al.*, Co-selection of antibiotic and metal resistance. *Trends in Microbiology* **14**, 176-182 (2006).
46. P. Kinnunen *et al.*, Local food crop production can fulfil demand for less than one-third of the population. *Nature Food* **1**, 229-237 (2020).
47. R. Gandolff, Lead exposure in childhood and historical land use: a geostatistical analysis of soil lead concentrations in South Philadelphia parks. *Environ Monit Assess* **195**, 356 (2023).
48. D. Huerta *et al.*, Probabilistic risk assessment of residential exposure to metal(loid)s in a mining impacted community. *Sci Total Environ* **872**, 162228 (2023).
49. M. A. Oliver, P. J. Gregory, Soil, food security and human health: a review. *European Journal of Soil Science* **66**, 257-276 (2015).
50. L. A. Naylor *et al.*, Stormy geomorphology: geomorphic contributions in an age of climate extremes. *Earth Surf Proc Land* **42**, 166-190 (2017).
51. A. Weber *et al.*, The risk may not be limited to flooding: polluted flood sediments pose a human health threat to the unaware public. *Environmental Sciences Europe* **35**, 58 (2023).
52. B. Tellman *et al.*, Satellite imaging reveals increased proportion of population exposed to floods. *Nature* **596**, 80-86 (2021).
53. J. R. Owen *et al.*, Catastrophic tailings dam failures and disaster risk disclosure. *International Journal of Disaster Risk Reduction* **42**, 101361 (2020).
54. L. Tang, T. T. Werner, Global mining footprint mapped from high-resolution satellite imagery. *Communications Earth & Environment* **4**, 134 (2023).
55. ICOLD, *Tailings Dams: Risk of Dangerous Occurrences : Lessons Learnt from Practical Experiences*. (Commission Internationale des Grand Barrages, 2001).
56. J. Liu *et al.*, A Bayesian Network-based risk dynamic simulation model for accidental water pollution discharge of mine tailings ponds at watershed-scale. *J Environ Manage* **246**, 821-831 (2019).
57. G. Z. Yin *et al.*, Stability analysis of a copper tailings dam via laboratory model tests: A Chinese case study. *Miner Eng* **24**, 122-130 (2011).
58. E. Lebre *et al.*, Source Risks As Constraints to Future Metal Supply. *Environ Sci Technol* **53**, 10571-10579 (2019).
59. E. Lebre *et al.*, The social and environmental complexities of extracting energy transition metals. *Nat Commun* **11**, (2020).
60. L. J. Sonter *et al.*, Renewable energy production will exacerbate mining threats to biodiversity. *Nat Commun* **11**, (2020).
61. D. M. Franks *et al.*, Tailings facility disclosures reveal stability risks. *Sci Rep-Uk* **11**, (2021).
62. J. Lewin, M. G. Macklin, "Metal mining and floodplain sedimentation in Britain." in *International Geomorphology Part 1,* V. Gardiner, Ed. (Wiley, 1986), pp. 1009-1027.

63. G. Bird *et al.*, Pb isotope evidence for contaminant-metal dispersal in an international river system: The lower Danube catchment, Eastern Europe. *Appl Geochem* **25**, 1070-1084 (2010).
64. G. Bird *et al.*, The solid state partitioning of contaminant metals and As in river channel sediments of the mining affected Tisa drainage basin, northwestern Romania and eastern Hungary. *Appl Geochem* **18**, 1583-1595 (2003).
65. G. Bird *et al.*, Heavy metal contamination in the Aries river catchment, western Romania: Implications for development of the Rosia Montand gold deposit. *J Geochem Explor* **86**, 26-48 (2005).
66. K. A. Hudson-Edwards *et al.*, The impact of tailings dam spills and clean-up operations on sediment and water quality in river systems: the Rios Agrio-Guadiamar, Aznalcollar, Spain. *Appl Geochem* **18**, 221-239 (2003).
67. M. P. Taylor, K. A. Hudson-Edwards, The dispersal and storage of sediment-associated metals in an and river system: The Leichhardt River, Mount Isa, Queensland, Australia. *Environ Pollut* **152**, 193-204 (2008).
68. G. Bird *et al.*, River system recovery following the Novat-Rosu tailings dam failure, Maramures County, Romania. *Appl Geochem* **23**, 3498-3518 (2008).
69. G. Bird *et al.*, The impact and significance of metal mining activities on the environmental quality of Romanian river systems. (2003), pp. 316-322.
70. G. Bird *et al.*, Quantifying sediment-associated metal dispersal using Pb isotopes: Application of binary and multivariate mixing models at the catchment-scale. *Environ Pollut* **158**, 2158-2169 (2010).
71. P. Byrne *et al.*, Water quality impacts and river system recovery following the 2014 Mount Polley mine tailings dam spill, British Columbia, Canada. *Appl Geochem* **91**, 64-74 (2018).
72. D. Ciszewski, Source of pollution as a factor controlling distribution of heavy metals in bottom sediments of Chechlo River (south Poland). *Environ Geol* **29**, 50-57 (1997).
73. K. A. Hudson-Edwards *et al.*, Sources, distribution and storage of heavy metals in the Rio Pilcomayo, Bolivia. *J Geochem Explor* **72**, 229-250 (2001).
74. A. R. Karbassi *et al.*, Metal pollution assessment of sediment and water in the Shur River. *Environ Monit Assess* **147**, 107-116 (2008).
75. M. G. Macklin, "Fluxes and storage of sediment-associated heavy metals in floodplain systems: assessment and river basin management issue as at a time of rapid environmental change." in *Floodplain processes*, M. G. Anderson, D. E. Walling, P. D. Bates, Eds. (Wiley, 1996), pp. 441-460.
76. M. G. Macklin *et al.*, "Review of the Porco Mine Tailings Dam Burst and Associated Mining Waste Problems, Pilcomayo Basin, Bolivia.", (1996)
77. W. M. Mayes *et al.*, Dispersal and Attenuation of Trace Contaminants Downstream of the Ajka Bauxite Residue (Red Mud) Depository Failure, Hungary. *Environ Sci Technol* **45**, 5147-5155 (2011).
78. J. N. Turner *et al.*, Heavy metals and As transport under low and high flows in the River Guadiamar three years after the Aznalcóllar tailings dam failure : implications for river recovery and management. *Cuad. Investig. Geográfica 28, 31 (2002).* **28**, 31-47 (2002).
79. V. Ettler *et al.*, Geochemical and Pb isotopic evidence for sources and dispersal of metal contamination in stream sediments from the mining and smelting district of Pribram, Czech Republic. *Environ Pollut* **142**, 409-417 (2006).

80. M. Gutierrez *et al.*, Mobility of Metals in Sediments Contaminated with Historical Mining Wastes: Example from the Tri-State Mining District, USA. *Soil Syst* **3**, (2019).
81. ICPDR, "Analysis of the Tisza River Basin 2007. Initial step toward the Tisza River Basin Management Plan", (2009) https://www.icpdr.org/main/sites/default/files/Tisza_RB_Analysis_2007.pdf.
82. C. G. Lee *et al.*, Heavy metal contamination in the vicinity of the Daduk Au-Ag-Pb-Zn mine in Korea. *Appl Geochem* **16**, 1377-1386 (2001).
83. J. S. Lee, H. T. Chon, Hydrogeochemical characteristics of acid mine drainage in the vicinity of an abandoned mine, Daduk Creek, Korea. *J Geochem Explor* **88**, 37-40 (2006).
84. M. G. Macklin *et al.*, The long term fate and environmental significance of contaminant metals released by the January and March 2000 mining tailings dam failures in Maramures County, upper Tisa Basin, Romania. *Appl Geochem* **18**, 241-257 (2003).
85. R. T. Pavlowsky *et al.*, Legacy sediment, lead, and zinc storage in channel and floodplain deposits of the Big River, Old Lead Belt Mining District, Missouri, USA. *Geomorphology* **299**, 54-75 (2017).
86. P. Renforth *et al.*, Contaminant mobility and carbon sequestration downstream of the Ajka (Hungary) red mud spill: The effects of gypsum dosing. *Sci Total Environ* **421**, 253-259 (2012).
87. J. N. Turner *et al.*, Fluvial-controlled metal and As mobilisation, dispersal and storage in the Rio Guadiamar, SW Spain and its implications for long-term contaminant fluxes to the Donana wetlands. *Sci Total Environ* **394**, 144-161 (2008).
88. W. J. F. Visser, "Contaminated Land Policies in Some Industrialised Countries ", (The Hague, 2500 GX, The Netherlands 1993) http://www.eugris.info/newsdownloads/WilmaVisserReport.pdf.
89. W. J. F. Visser, Contaminated Land Policies in Europe. *Chem Ind-London*, 496-499 (1995).
90. D. Yamazaki *et al.*, A high-accuracy map of global terrain elevations. *Geophys Res Lett* **44**, 5844-5853 (2017).
91. F. Nardi *et al.*, GFPLAIN250m, a global high-resolution dataset of Earth's floodplains. *Sci Data* **6**, (2019).
92. P. Scussolini *et al.*, Global River Discharge and Floods in the Warmer Climate of the Last Interglacial. *Geophys Res Lett* **47**, 1-12 (2020).
93. S. Siebert *et al.*, "Update of the Digital Global Map of Irrigation Areas to Version 5", (2013) https://www.fao.org/3/I9261EN/i9261en.pdf.
94. W. Schwanghart, D. Scherler, Short Communication: TopoToolbox 2-MATLAB-based software for topographic analysis and modeling in Earth surface sciences. *Earth Surf Dynam* **2**, 1-7 (2014).
95. H. Leenaers, *The dispersal of metal mining wastes in the catchment of the river Geul (Belgium - The Netherlands)*. (Utrecht, 1989), pp. 230.
96. P. A. Brewer *et al.*, "The use of geomorphological mapping and modelling for identifying land affected by metal contamination on river floodplains. ", (2003)
97. K. A. Hudson-Edwards *et al.*, "Assessment of metal mining-contaminated river sediments in England and Wales", (Environment Agency,2008)
98. ESDAT, "Circular on target values and intervention values for soil remediation.", www.esdat.net.

99. P. Ashton *et al.*, “An overview of the impact of mining and mineral processing operations on water resources and water quality in the Zambezi, Limpopo and Olifants catchments in southern Africa”, (CSIREnvironmentek, Pretoria, South Africa and Geology Department, University of Zimbabwe, Harare, Zimbabwe,2001) https://iied.org/sites/default/files/pdfs/migrate/G02404.pdf.
100. M. C. W. Lourens, T, D., “Operating Mines and Quarries and Mineral Processing 203 Plants in the Republic of South Africa (Directory D1/2016). ”, (2016) https://www.resourcedata.org/dataset/rgi-operating-mines-and-quarries-and-mineral-processing-plants-in-the-republic-of-south-africa-2016.
101. P. Chuhan-Pole *et al.*, *Mining in Africa: Are Local Communities Better Off?* , Mining in Africa: Are Local Communities Better Off? (The World Bank, 2017).
102. Deloitte, “Industry Outlook Mining in Argentina.”, (2016) https://www2.deloitte.com/content/dam/Deloitte/ar/Documents/finance/Industry%20Outlook%20-%20Mining%20in%20Argentina.pdf.
103. Australian Government, “Australian Mines Atlas”, https://portal.ga.gov.au/persona/minesatlas.
104. T. T. Werner *et al.*, A Geospatial Database for Effective Mine Rehabilitation in Australia. *Minerals-Basel* **10**, (2020).
105. “Government of The Wallonia - Brussels Federation”, https://www.arcgis.com/home/webmap/viewer.html?featurecollection=https%3A%2F%2Fgeoservices.wallonie.be%2Farcgis%2Frest%2Fservices%2FSOL_SOUS_SOL%3Ff%3Djson%26option%3Dfootprints&supportsProjection=true&supportsJSONP=true.
106. L. J. Sonter *et al.*, Renewable energy production will exacerbate mining threats to biodiversity. *Nat Commun* **11**, 1-6 (2020).
107. Hudson Institute of Mineralogy, “Mines, Minerals and More”, https://www.mindat.org/.
108. “National Mining Dams Registry”, http://www.anm.gov.br/assuntos/barragens/pasta-cadastro-nacional-de-barragens-de-mineracao/cadastro-nacional-de-barragens-de-mineracao .
109. SeeNews, “Gold Mining and Processing in Bulgaria”, (2010); https://seenews.com/reports/industry_report/gold-mining-and-processing-bulgaria-2010-58.
110. Government of Canada, “Principal mineral areas, producing mines, and oil and gas fields in Canada / Lands and Minerals Sector and National Energy Board ”, (2021); https://publications.gc.ca/site/eng/9.853130/publication.html.
111. Media Edge Publishing, “Ontario Mining & Exploration Directory - 2021”, (2021); https://www.mndm.gov.on.ca/en/news/mines-and-minerals/ontario-mining-exploration-directory-2021.
112. B. G. Wei, L. S. Yang, A review of heavy metal contaminations in urban soils, urban road dusts and agricultural soils from China. *Microchem J* **94**, 99-107 (2010).
113. Z. Y. Li *et al.*, A review of soil heavy metal pollution from mines in China: Pollution and health risk assessment. *Sci Total Environ* **468**, 843-853 (2014).
114. H. Y. Chen *et al.*, Contamination features and health risk of soil heavy metals in China. *Sci Total Environ* **512**, 143-153 (2015).
115. X. M. Chen *et al.*, Speciation and distribution of mercury in soils around gold mines located upstream of Miyun Reservoir, Beijing, China. *J Geochem Explor* **163**, 1-9 (2016).
116. X. W. Zhang *et al.*, Impacts of lead/zinc mining and smelting on the environment and human health in China. *Environ Monit Assess* **184**, 2261-2273 (2012).

117. J. Pinedo-Hernandez *et al.*, Speciation and bioavailability of mercury in sediments impacted by gold mining in Colombia. *Chemosphere* **119**, 1289-1295 (2015).
118. "Cuba Economic Activity Map 1977", https://www.gifex.com/cuba_maps/Cuba_Economic_Activity_Map_2.htm.
119. V. Štrupl *et al.*, Current state of registered hazardous abandoned mine waste facilities in the Czech Republic. *Geoscience Research Reports* **50**, 95-97 (2017).
120. M. L. Räisänen *et al.*, "Suljettujen ja hylättyjen kaivosten kaivannaisjätealueiden kartoitus. (Mapping of mine waste areas in closed and abandoned mines)", (2013) https://helda.helsinki.fi/bitstream/handle/10138/41486/YMra_24_2013.pdf?sequence=1&isAllowed=y.
121. K. Nasri *et al.*, Unlikely lead-bearing phases in river and estuary sediments near an ancient mine (Huelgoat, Brittany, France). *Environ Sci Pollut R* **28**, 8128-8139 (2021).
122. Federal Institute for Geosciences and Natural Resources, "Map of Mining and Storage Operations of the Federal Republic of Germany 1 : 2 000 000 (BergSP)", https://www.bgr.bund.de/EN/Themen/Sammlungen-Grundlagen/GG_geol_Info/Karten/Deutschland/Kt_Bergbau/bergSP_inhalt_en.html?nn=1556480.
123. Mining and Geological Survey of Hungary, "Mining areas in Hungary", (2022); https://mbfsz.gov.hu/en/node/408.
124. Ministry of Mines. Government of India, "Mineral Map of India", https://www.mines.gov.in/UserView/index?mid=1272.
125. EPA Ireland, "EPA GeoPortal - Historic Mines project", https://gis.epa.ie/GetData/Download.
126. Istituto Superiore per la Protezione e la Ricerca Ambientale, "Database cave e miniere servizio geologico d'Italia - GEMMA", https://www.isprambiente.gov.it/it/progetti/cartella-progetti-in-corso/suolo-e-territorio-1/miniere-e-cave/progetto-remi-rete-nazionale-dei-parchi-e-musei-minerari-italiani/banche-dati/database-nazionale-cave-miniere-servizio-geologico-d2019italia.
127. V. Bogdetsky, V. Novikov, "Mining, development and environment in Central Asia: Toolkit Companion with case studies", (2012) https://wedocs.unep.org/handle/20.500.11822/7549.
128. Central Asian Geoportal, "Geological and mineral resources map ", https://cac-geoportal.org/.
129. P. Kyophilavong, "Mining Sector in Laos" in *BRC Discussion Paper Series No. 18, Edition 1*, I.-J. Bangkok Research Center (BRC), Ed. (Bangkok Research Center (BRC), 2009), pp. 69-100.
130. University of Texas, "Mexico Mining and Industry", https://maps.lib.utexas.edu/maps/americas/mexico_industry_1978.jpg.
131. Geo-Mexico, "The geography of gold mining in Mexico", (2013); https://geo-mexico.com/?p=9658.
132. N. J. Gardiner *et al.*, The metallogenic provinces of Myanmar. *Applied Earth Science* **123**, 25-38 (2014).
133. N. J. Gardiner *et al.*, Tin mining in Myanmar: Production and potential. *Resour Policy* **46**, 219-233 (2015).
134. E. B. Eckel *et al.*, "Geology and mineral resources of Paraguay--a reconnaissance, with sections on Igneous and metamorphic rocks and soils", *Professional Paper* (1959) http://pubs.er.usgs.gov/publication/pp327.

135. PWC, "Doing Business in Peru - Mining Chapter", (2020) https://www.pwc.pe/es/publicaciones/assets/PwC-Doing-Business-in-Peru-Mining.pdf.
136. A. van Geen *et al.*, Lead exposure from soil in Peruvian mining towns: a national assessment supported by two contrasting. examples. *B World Health Organ* **90**, 878-886 (2012).
137. LNEG, "Portugal - Exploration and Mining", (2000) https://geoportal.lneg.pt/pt/bds/siorminp#!/.
138. European Commission, "Extractive Waste - Closed and abandoned waste facilities (2017).", (2017); https://www.economie.gov.ro/images/legislatie/Resurse%20Minerale/Inventar_Iazuri_de_Decantare_iulie_2012.pdf.
139. T. R. Walker *et al.*, Anthropogenic metal enrichment of snow and soil in north-eastern European Russia. *Environ Pollut* **121**, 11-21 (2003).
140. J. Jarsjo *et al.*, Patterns of soil contamination, erosion and river loading of metals in a gold mining region of northern Mongolia. *Reg Environ Change* **17**, 1991-2005 (2017).
141. J. Monthel *et al.*, "Mineral deposits and mining districts of Serbia - Compilation map and GIS databases", (2002) http://gras.org.rs/wp-content/uploads/2017/10/mineral-deposits-and-mining-districts-of-serbia.pdf.
142. N. Atanackovic *et al.*, Regional-scale screening of groundwater pollution risk induced by historical mining activities in Serbia. *Environ Earth Sci* **75**, (2016).
143. Slovak Environment Agency "Information system on extractive waste management", https://app.sazp.sk/Odpady_tp/About.aspx.
144. M. Gosar *et al.*, "Preparation of a list of enclosed facilities for the management of waste from mining and other mineral resource mining activities : report of the 3rd phase of the project. (Geological Survey of Slovenia, 2014).", (2014)
145. T. Assawincharoenkij *et al.*, Mineralogical and geochemical characterization of waste rocks from a gold mine in northeastern Thailand: application for environmental impact protection. *Environ Sci Pollut R* **25**, 3488-3500 (2018).
146. X. Li *et al.*, Recent evolution of the Mekong Delta and the impacts of dams. *Earth-Sci Rev* **175**, 1-17 (2017).
147. D. Potter, D. Johnston, "Inventory of closed mining waste facilities", (Environment Agency,2014) https://assets.publishing.service.gov.uk/government/uploads/system/uploads/attachment_data/file/288582/LIT_6797_7d390c.pdf.
148. F. Santos-Frances *et al.*, Distribution and mobility of mercury in soils of a gold mining region, Cuyuni river basin, Venezuela. *J Environ Manage* **92**, 1268-1276 (2011).
149. P. G. Schruben *et al.*, "Geology and mineral resource assessment of the Venezuelan Guayana Shield at 1:500,000 scale; a digital representation of maps published by the U.S. Geological Survey", (USGS,1997) https://pubs.usgs.gov/dds/dds46/.
150. M. M. B. Veiga, D. *et al.*, "Mercury Pollution from Artisanal Gold Mining" in *Dynamics of Mercury Pollution on Regional and Global Scales*, N. Pirrone, K. R. Mahaffey, Eds. (Springer, Boston, MA, 2005), pp. 421-450.
151. United States Government, "U. S. Government open data portal", https://catalog.data.gov/dataset?tags=mines.
152. L. N. Bowker, D. M. Chambers, "The Risk, Public Liability, and Economics of Tailings Storage Facility Failures. 2015. ", (2015) http://www.csp2.org/files/reports/Bowker%20%26%20Chambers%20-%20Risk-

Public%20Liability-Economics%20of%20Tailings%20Storage%20Facility%20Failures%20%E2%80%93%2023Jul15.pdf.

153. Q. T. Li *et al.*, Detection of Tailings Dams Using High-Resolution Satellite Imagery and a Single Shot Multibox Detector in the Jing-Jin-Ji Region, China. *Remote Sens-Basel* **12**, (2020).

154. L. Tang *et al.*, Statistical analysis of tailings ponds in China. *J Geochem Explor* **216**, (2020).

Acknowledgments:

MGM is grateful to the University of Lincoln for supporting the Lincoln Centre for Water and Planetary Health by funding AM's and KRM's PDRA posts.

Funding: University of Lincoln (AM, KRM)

Author contributions:

Conceptualization: MGM

Methodology: CJT, MGM, AM, JL, PAB

Investigation: AM, KRM, MGM, AL, PAB, JO, GB, DK

Visualization: AM, MGM, CJT, PS, DE

Funding acquisition: MGM

Project administration: MGM, CJT

Supervision: MGM, CJT

Writing – original draft: MGM

Writing – review & editing: MGM, CJT, AM, PAB, KAH-E, JL, PS, DE, AL, JO, GB, DK, KRM

Competing interests: The authors declare no competing interests.

Data and materials availability:

The Water and Planetary Health Analytics (WAPHA) global metal mines database is divided into four components. Publicly available data on (i) active and (ii) inactive metal mines are available from the United States Geological Survey Mineral Resources Data System (*31*) (https://mrdata.usgs.gov/mrds/), BritPits database of the British Geological Survey (*32*) (https://www.bgs.ac.uk/datasets/britpits/), and the S&P Global Market Intelligence database (*33*) (https://www.spglobal.com/marketintelligence/en/campaigns/metals-mining). In addition, data for c. 100,000 additional active/inactive mines, obtained from academic and gray literature, are stored in the WAPHA database (*29*) (https://doi.org/10.5061/dryad.j3tx95xmg). Publicly available data relating to (iii) tailings storage facilities, and (iv) tailings dam failures, are available from: ICOLD/UNEP (*34*) (https://books.google.co.uk/books?id=8W0hAQAAIAAJ), the World Information Service on Energy (*35*) (https://wise-uranium.org/mdaf.html), the World Mine Tailings Failures and Global Tailings Portal databases (*36*) (https://tailing.grida.no/). Additional TSF/TDF data, obtained from academic and gray literature, are stored in the WAPHA database (*29*) (https://doi.org/10.5061/dryad.j3tx95xmg). Modelling was implemented procedurally in MATLAB v9.9.0 (R2020b) (*37*) with the open source TopoToolbox MATLAB program for the analysis of digital elevation models (https://topotoolbox.wordpress.com). Modelling workflow is presented in SI Figure S8 with example code available in the WAPHA database (*29*) (https://doi.org/10.5061/dryad.j3tx95xmg).

Supplementary Materials:

Materials and Methods

Figs. S1 to S12

Tables S1 to S17

References (54 - 154)

Fig 1. Global distribution (Equal Earth projection) of: A) inactive metal mines (solid blue circles), B) active metal mines (solid red circles), C) number of active/inactive mines by continent, D) tailing storage facilities (blue triangles intact, red triangles failed), and E) number of intact and failed tailings storage facilities (TSF) by continent. Disaggregated on a continental scale, North America (active 11,871; inactive 80,995) and Oceania (active 3,430; inactive 53,233) have the largest number of mines followed by South America (active 3,240; inactive 14,577), Europe (active 1,024; inactive 9,080), Asia (active 1,817; inactive 1,473), and Africa (active 1,227; inactive 377) (table S1). Oceania, Europe, North America, and South America are mostly affected by inactive mining, while active mining activities are more important in Africa and Asia (table S1). We recorded 11,844 TSF, of which 257 had failed. Asia has nearly half of the world's TSF with North America recording both in absolute (107) and proportional (42%) terms the largest number of tailings dam failures (table S4).

Fig. 2. Global river length, floodplain and 100-year flood inundation area affected by metal mines (inactive mines shown by solid yellow circles; active mines shown by open red circles) and failed tailings storage facilities (purple triangles). Y-axis units are Log10 numbers. Symbols for inactive and active mines indicate predicted values from the WAPHA model with 90% confidence intervals; symbols for failed tailing storage facilities are observed values for total river length and floodplain areas affected by 257 documented TDFs. Inactive metal mines have a significantly larger global environmental impact on river channels, floodplains and valley floors located within the 100-year inundation zone than active mines. Although the impact of failed tailings storage facilities on river systems worldwide is significant, the combined environmental effect of inactive and active mines on river channels and floodplains is estimated to be 30-90 times larger.

Fig 3. Human population, number of livestock (cattle, goat, sheep) and the area of irrigated land affected by metal mines (inactive mines shown by solid yellow circles; active mines shown by open red circles) and failed tailings storage facilities (purple triangles). Y-axis units are Log_{10} numbers. Symbols for inactive and active mines indicate predicted values from the WAPHA model with 90% confidence intervals; symbols for failed tailing storage facilities are observed values for irrigated areas (km^2) affected by 257 documented TDFs.

Fig 4. Examples of WAPHA modelling and mapping of contaminated floodplains and river channel reaches linked to inactive and active mines in: B) River Swale, northern England, and D) Bulgaria. A) and C) show regional index maps for the UK and Eastern European sites, respectively. Yellow solid circles show the location of inactive mines and red open circles show the location of active mines. The stream network is shown by blue lines and floodplains denoted in hatched black fill. Contaminated river channel reaches and floodplains are delineated in red (contamination from a mine to the distance given by the lower confidence interval), deep pink (contamination beyond the lowest confidence interval extending to the distance predicted by the model) and light pink (contamination beyond the predicted distance extending to the upper confidence interval).

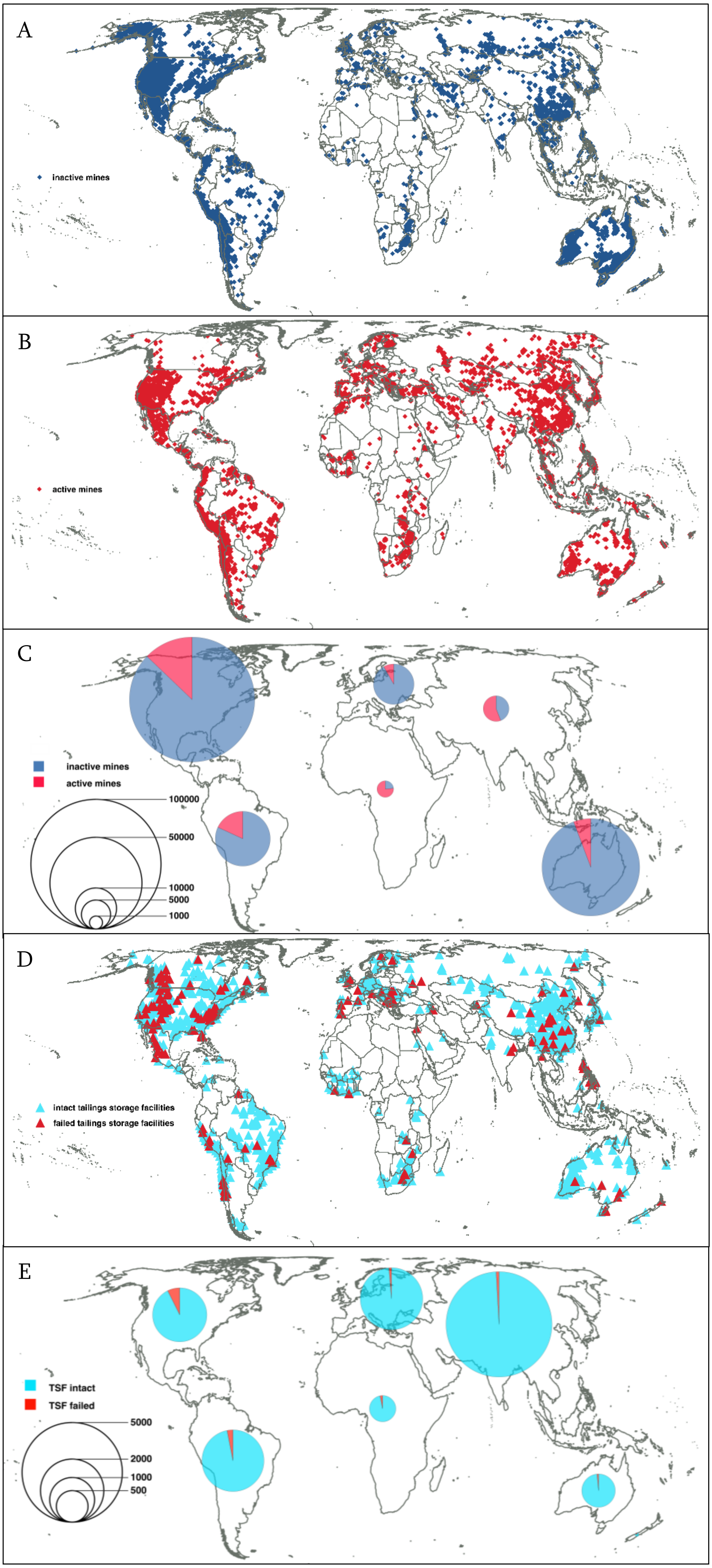
A
inactive mines
B
active mines
C
inactive mines
active mines
100000
50000
10000
5000
1000
D
intact tailings storage facilities
failed tailings storage facilities
E
TSF intact
TSF failed
5000
2000
1000
500

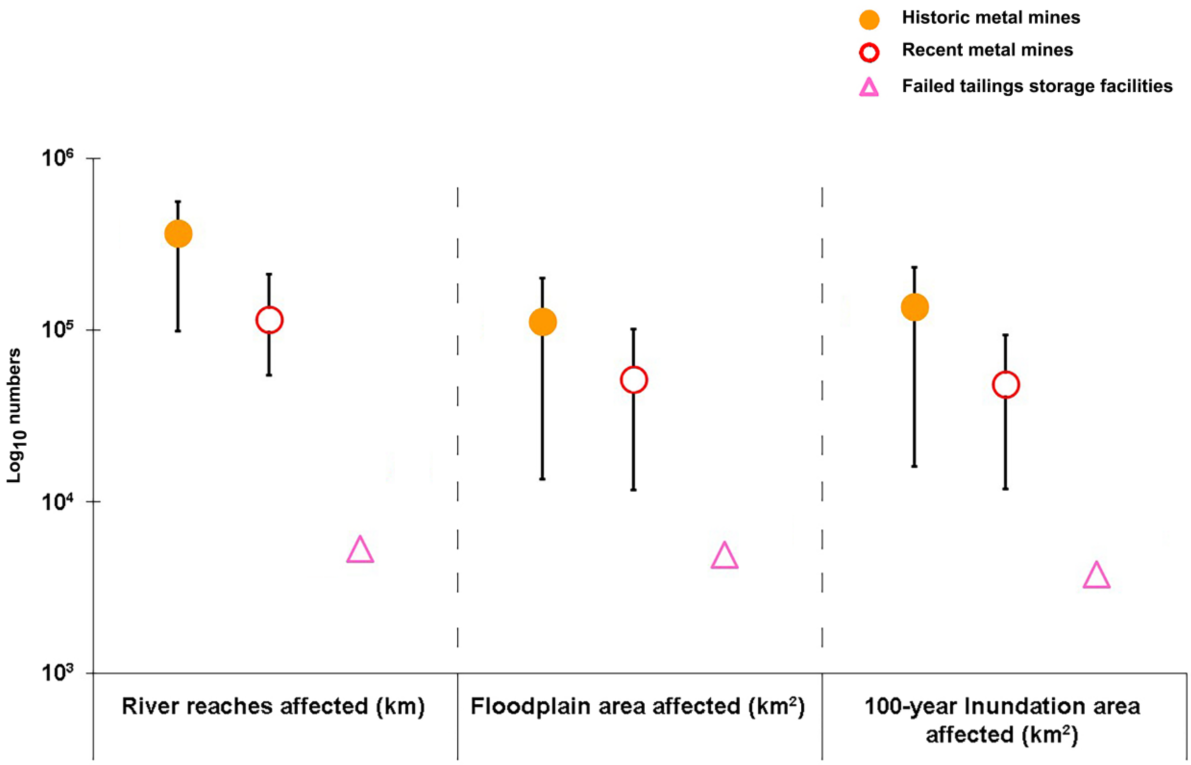

Historic metal mines
Recent metal mines
Failed tailings storage facilities
10^6
10^5
10^4
10^3
Log_{10} numbers
River reaches affected (km)
Floodplain area affected (km^2)
100-year Inundation area affected (km^2)

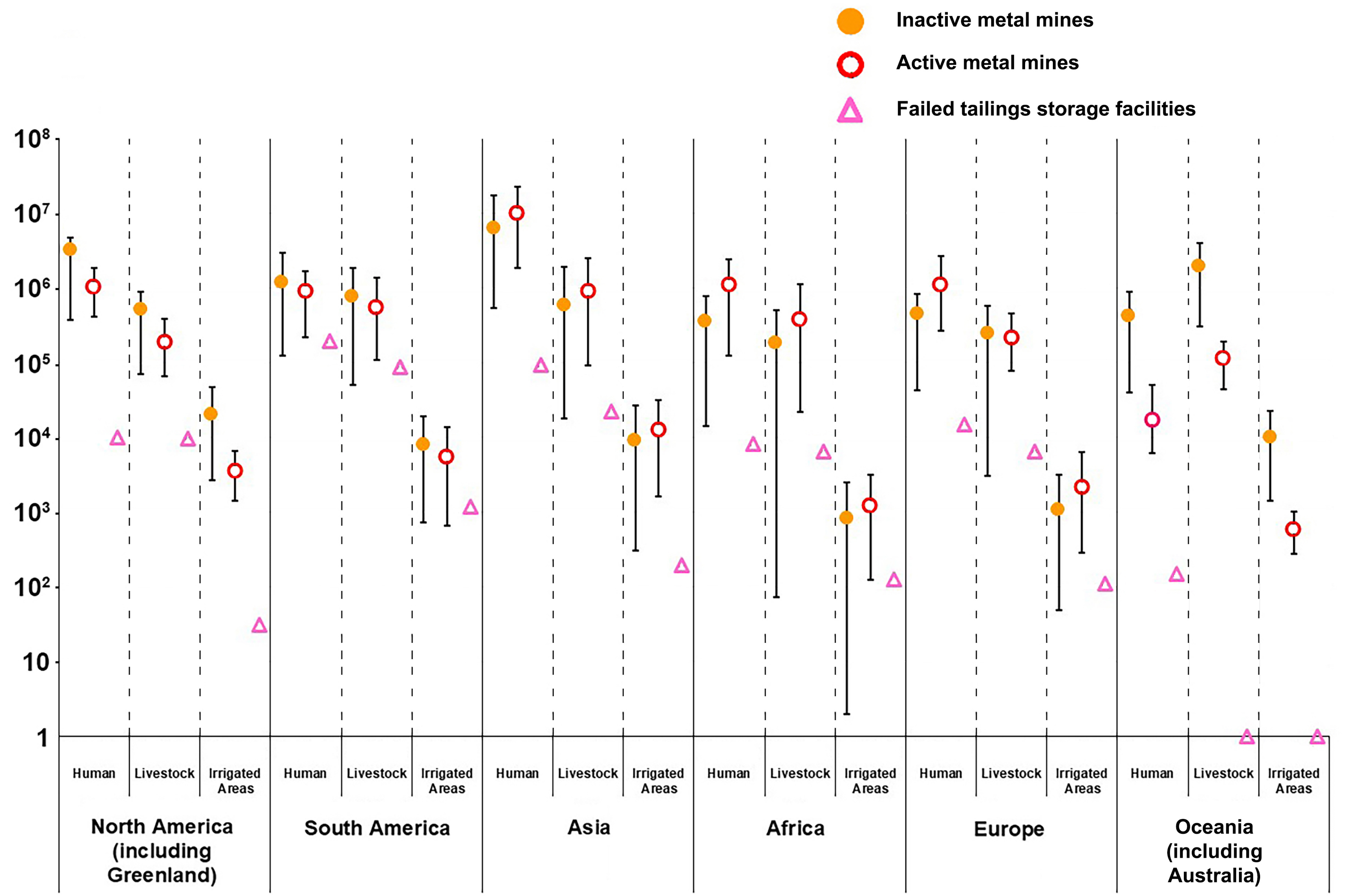

Inactive metal mines
Active metal mines
Failed tailings storage facilities
10^8
10^7
10^6
10^5
10^4
10^3
10^2
10
1
Human
Livestock
Irrigated Areas
North America (including Greenland)
South America
Asia
Africa
Europe
Oceania (including Australia)

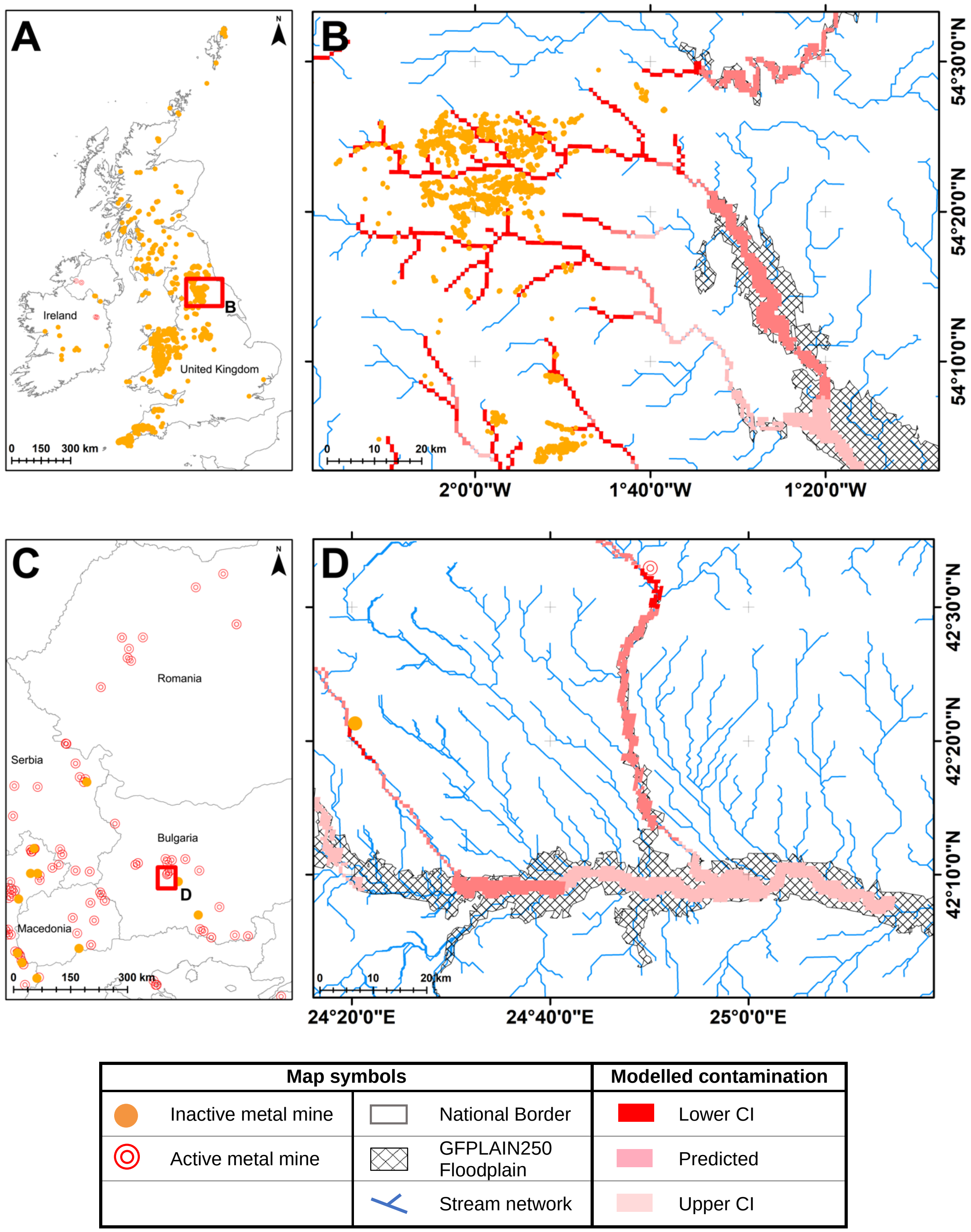

A
N
Ireland
United Kingdom
B
0 150 300 km
B
54°30'0"N
54°20'0"N
54°10'0"N
2°0'0"W
1°40'0"W
1°20'0"W
0 10 20 km
C
N
Romania
Serbia
Bulgaria
D
Macedonia
0 150 300 km
D
42°30'0"N
42°20'0"N
42°10'0"N
24°20'0"E
24°40'0"E
25°0'0"E
0 10 20 km
Map symbols
Inactive metal mine
Active metal mine
National Border
GFPLAIN250 Floodplain
Stream network
Modelled contamination
Lower CI
Predicted
Upper CI

Science
AAAS

Supplementary Materials for

Impacts of metal mining on river systems: a global assessment

M.G. Macklin, C.J. Thomas, A. Mudbhatkal, P.A. Brewer, K.A. Hudson-Edwards, J. Lewin, P. Scussolini, D. Eilander, A. Lechner, J. Owen, G. Bird, D. Kemp, K. R. Mangalaa.

Correspondence to: mmacklin@lincoln.ac.uk

This PDF file includes:

Materials and Methods
Figs. S1 to S12
Tables S1 to S17
References

Materials and Methods

<u>Development of the Water and Planetary Health Analytics (WAPHA) global metal mines, tailings storage facilities and tailings dam failure database</u>

Our new global metal mines database comprises information, published/accessed before August 29th 2022, from the United States Geological Survey's Mineral Resources Data System (MRDS) *(24)* (73,917 mines worldwide), the BritPits survey of the British Geological Survey (*25*) (8,459 mines in the United Kingdom), the S&P Global Market Intelligence database (*26*) (2,584 mines worldwide), and our own compilation of c. 100,000 additional mines from the worldwide academic and grey literature, including regional data published by government agencies and industry (tables S1-S2). Twenty-one types of active and inactive metal and metalloid mines were used in our modelling and analysis (tables S3a-S3b). In total, the new georeferenced metal mines database contains 22,609 active and 159,735 inactive mines spread across six continents. It is noteworthy that our mapped global distribution of active mines (Fig 1A) from these archive sources is highly consistent with that recently reported from mapping mines by remote sensing (*42*).

Data on tailings storage facilities (TSFs) and tailings dam failures (TDFs) were obtained from peer-reviewed academic articles and from grey literature published by government and private agencies (tables S2, S4). Search terms used included: tailings storage facilities; tailings dam failures; mine tailings ponds; tailings dam spills and clean-up operations; tailings dam burst; metal mining. The data were augmented using the WISE database (*28*); ICOLD/UNEP 2001 compilation (Bulletin 121) (*43*); a database provided for years 1915 to 2019 by Center for Science in Public Participation, Global Tailings Portal (*29*); and personal communication with Dr Jeannette Meima (Federal Institute for Geosciences and Natural Resources (BGR), Germany), Lindsay Newland Bowker (Bowker Associates Science and Research in The Public Interest), and Paulina Concha Larrauri (Columbia University). A key component of our data checking was visual confirmation and geo-referencing of all TSFs and TDFs using Google Earth. The WAPHA's georeferenced global database of TSFs and TDFs holds data on 11,587 TSFs and 257 recorded TDFs (table S5). This is undoubtedly an underestimate as data are not publicly available in India and Russia (*44, 45*). Information on the production capacity of mines, the start year of production/tailings storage facilities, year of closure (in case of mines/tailings storage facilities), dam height and input volume of tailings (for estimating runout from intact tailings storage facilities) where available are included in the source database.

<u>Comparison of WAPHA global metal mines database with S&P Global Market Intelligence database and Global Tailings Portal</u>

To assess the completeness of the WAPHA database we compare the distribution of the metal mines and tailings storage facilities with two existing and well-known global databases. A comparison of the metal mines in the S&P Global Market Intelligence database (*26*) and the WAPHA database is shown in tables S3a-S3b, and tailings storage facilities in the Global Tailings Portal (GTP) (*29*) and the WAPHA database is presented in Table S5. The comparisons between the WAPHA, the S&P and GTP databases provide an assessment of the WAPHA's completeness, a key dimension of spatial data quality. The S&P dataset, which was also integrated into the WAPHA database, is one of the few global mining datasets that has been used in similar global spatial assessments of mining related societal and/or environmental impacts (*46-48*). Even though the S&P dataset has demonstrated utility for supporting global analyses, the WAPHA contains ten times more metal mines. The S&P dataset only represented 0.5% and 8% of the inactive and active mines in the WAPHA database, respectively (table S1). However, the S&P dataset was an important source for identifying that inactive mines in Africa and active mines in Asia, account for 14% and 54% of the mines in these regions in the WAPHA database, respectively. The more recent GTP database has also been utilized in a similar global assessment (*49*), but it only represents 30% of the total tailings storage facilities in the WAPHA database (Table S5). The GTP database was found to be relatively complete for Africa and Asia accounting for 97% and 86% of WAPHA database tailing storage facilities, respectively. The WAPHA database represents a step change in the available mine and tailing storage facility spatial data for analyzing global patterns.

The WAPHA's process-based global model of sediment-associated mining contaminant dispersal

Field-based measurements collected and published over the last 40 years or so (*13*, *15-21*, *50*) indicate that concentrations of sediment-associated contaminant metals and metalloids in rivers attenuate with distance from mining operations. This is due primarily to dilution and mixing with relatively 'clean' non-mining sediments, and to a more limited extent by hydraulic sorting (*13*). To predict the extent of river contamination downstream from metal mines globally, we have developed a simple, process-based model of contaminant metal (Cu, Pb and Zn) and metalloid (As) dispersal and attenuation from individual metal mines. This selection of elements was determined by data availability in river systems worldwide, where As, Cu, Pb and Zn concentrations in sediments tend to be routinely measured in environmental geochemical assessments.

Metal contamination attenuation downstream from mines

Observed concentrations of As, Cu, Pb and Zn in overbank (<0.063 mm, <1 mm and <2 mm) and channel sediments (<0.063 mm, <1 mm, <2 mm), along with downstream distance from the mine that was the source of contamination, were extracted from an extensive global review of rivers affected by inactive or actively active metal mining *(18, 20, 21, 51-76)*. To generate a statistically skilled and widely applicable model of sediment-associated metal and metalloid dispersal, only studies that had collected geochemical data downstream from a single mining source were used in our analyses. This resulted in 739 sample points, from 79 locations (44 in the Northern Hemisphere and 35 in the Southern Hemisphere) in 33 rivers with catchment areas ranging from 46-232,000 km^2. These data incorporate six different Köppen-Geiger (KG) climate zones (BSh - hot semi-arid; BSk - cold semi-arid; Cfa - humid subtropical climate; Cfb – temperate oceanic; Cwa - monsoon-influenced humid subtropical; Dfb - warm-summer humid continental) and are representative of the range of regions included in subsequent modelling.

Globally and historically, various contaminant metal and metalloid intervention values for soil remediation at sites affected by metal mining have been set (see *(21)* for a review). These indicate the concentration levels of metals, or metalloids, above which the functionality of soil for human, plant, and/or animal life may be seriously compromised or impaired *(77, 78)*. For this global assessment of river contamination, we use the Dutch intervention values (table S6), on the basis that the Netherlands has one of the longest histories of soil/sediment protection policy dating back to 1962 *(77)*, and guidelines were reformulated in the mid-1990s using eco-toxicological methods based upon potential exposure routes to people. In the case for Pb, we use sediment concentrations that exceed 530 mg/kg to delineate the extent of contamination and its likely impact on ecosystem and human health downstream from a mine. Figure S1 shows the plot of reported Pb concentrations up to 50 km downstream of individual mine sites in our database. The data exhibited a wide spread of initial concentrations (figure S2) with a minimum concentration of 68 mg/kg, maximum concentration of 49,092 mg/kg and mean of 5,745 mg/kg (mines n=79).

Model for downstream dispersal of sediment-associated contaminant metal and metalloid

Initial data exploration of processes was conducted with Pb, for which the largest sample size was available. The Pb concentration and downstream distance from the mine sites were log transformed to normalize the data and establish linearity for univariate ANOVA and Generalised Linear Model regression. There were no significant differences in logPb vs logD by KG climate zone (F (7, 622) =0.019, p=0.942), sediment type (channel vs overbank F (1,629) =2.341, p=0.369), or catchment area (F (1,550) =0.288, p = 0.593). To evaluate the variance in attenuation of Pb from each mine in relation to initial concentration, the concentrations downstream from each mine series were converted to proportions of the initial concentration at the mine with each series therefore starting at Pb proportion = 1 at distance = 0 (figure S3). While most downstream points declined by distance from the mine, we observed some downstream points increasing in concentration. For example, three downstream concentrations exceeded 1, which may be attributed to additional contamination sources (e.g., erosion of historically contaminated floodplain sediment downstream of the mine, or additional input from streams joining between sample locations).

GLM regression predicting log Pb by log (D+1) was highly significant and explained some 26% of observed variation (R^2 = 0.259, F (1,737) = 257, p <0.001). Cu (R^2 = 0.059, F (1,249) = 15.7, p <0.001), Zn (R^2 = 0.137, F (1,704) = 111.0, p <0.001), and As (R^2 = 0.267, F (1,38) = 13.8, p <0.001) followed similar trends. We interpret remaining variance to be due to local factors that are presently not quantifiable at the global scale. Based on typical element associations found within the main mineral commodity at any given mine (table S7), we have used downstream attenuation rates from one or more of these elements (As, Cu, Pb, Zn) to model and estimate the downstream extent of contamination from that specific mine.

We used the Dutch Intervention Limits (DIL) as the threshold for safe concentration levels of contaminant metals. Using non-linear modelling tools in MATLAB, we found a 2-parameter negative exponential model gave the best fit to the empirical data of reported concentration by distance along the river from a mine (point source) for Pb (the element with the largest sample size from the literature) (figure S3). Given this relationship, the global threshold distance downstream from a mine at which the DIL concentration would occur for each of As, Cu, Pb and Zn was estimated by fitting a 2-parameter negative exponential regression model. This model was derived from empirical data reported for each element, predicting distance from mine by observed concentration, as the goal was to estimate the DIL threshold distance (Eqn. 1)

Eqn. 1. $\text{Distance} = A * \exp^{(B*\text{concentration})}$

where A and B are estimated parameters. Results of modelling are presented in table S6 and figures S4-S7. Confidence intervals were estimated at 95% for all metals but for As we could only estimate reasonably with confidence at 90% due to the smaller sample size.

Sources of data for spatial global contamination modelling

In addition to the new WAPHA database, variables were derived from spatially explicit high-resolution global data sets:

Hydrologic and geomorphic data sources:

- Hydrologically corrected MERIT Digital Elevation Model, which represents terrain elevations at 0.00083° resolution with available extent 90°N-60°S, to delineate the river network and for modelling metal mining affected reaches *(79)*;
- Watershed boundaries derived from the HydroBASINS *(31)*; at 0.004167° resolution gridded global floodplains, GFPLAIN250 *(80)*, 250m resolution with available extent 60°N-60°S and 139W to 180E;
- Gridded, global 100-year flood areas at 0.005° resolution with global extent *(81)*.

Demographic and livestock databases:

- SEDAC gridded population for the year 2020, at 0.0083° resolution GPW (v.33) *(33)*.
- FAO Gridded Livestock of the World GLW3 2010 (cattle, goat and sheep), at 0.0083° resolution (v.34) *(34)*.
- Gridded Global Map of Irrigation Areas GMIA, at 0.0083° resolution *(82)*.

The WAPHA model of metal mining impacts on river systems at a global scale

Modelling was implemented in MATLAB (MATLAB. (2020) version 9.9.0 (R2020b) *(30)* with TopoToolbox (*83*). We opted for a DEM grid-based approach, rather than using in-built routing through published vector stream networks such as MERIT Hydro streams or HydroRIVERS, to create a process that is applicable independent of the DEM, enabling future research at different scales. The WAPHA model framework and workflow is presented in figure S8 and is illustrated through the maps in figures S9-S12, for representative catchments in the UK, Central Europe (Romania and Bulgaria), South America (Brazil and Peru) and Central Asia (Turkmenistan, Uzbekistan, Kazakhstan and Kyrgyzstan).

The use of basin polygons was for computational efficiency, specifically to reduce the size of the DEM used in calculations to the extent of level 4 basin polygon bounding box, each one considered in turn, and to allow projection to local UTM for metric measurements. Prior to analysis we assessed the optimal HydroBasins level, and level 4 was both tractable for efficient computation yet large enough to encompass downstream contamination, as almost all metal mines are situated in the upper reaches of these basins and stream networks. Of the 22,609 active mines, 10,021 were located in basins which had outflow into another basin. Mines tended to be located in the upper reaches of a catchment. Computing the distance downstream along our calculated stream network from the MERIT DEM to the boundary of the HydroBasin for each of these mines, we found only 14 mines who's contaminated runout by commodity was truncated at the basin boundary. The 'lost' contamination runout was 341 km, that is, 0.3% of the 114,000 km global total. We considered this well within the error of our global estimate, and did not warrant the complexity of extending contamination into receiving catchments.

For each global catchment in the HydroBASINS level 4 polygons (corresponding to Pfafstetter level 4, polygons derived from 15 arc second resolution HydroSHEDS DEM), we determined if any active or inactive mines in the WAPHA database were located within it using spatial overlay. If a catchment contained mines, the rectangular extent defined by the catchment bounding box was extracted from the hydrologically corrected MERIT DEM (3 arc second resolution) and re-projected from spherical coordinates into local UTM at 500m resolution, to enable calculation of distances and areas in metric units with minimal map distortion. Using TopoToolbox functions, we defined the catchment stream network from the MERIT DEM using a minimum upstream contributing area of 10 km^2 (figure S8). We calculated the stream network locations nearest to each mine and, for each metal/metalloid relevant to that mine, we defined all downstream grid cells in the basin within the attenuation distances as contaminated areas at predicted, upper and lower confidence levels. Results from each mine were combined to map the cumulative contaminated grid cells along flow paths (figure S10). The catchment extent was also extracted from the global floodplain (GFPLAIN250, 250m resolution) and global 100-year flood grids (0.005° resolution) gridded data and re-projected to local UTM at 500 m resolution. Contaminated stream grid cells in floodplains were delineated in two ways: first, using a buffer based on empirical data *(21, 84)* showing that metal and As concentrations in overbank sediments do not generally exceed DIL more than 500 m from river channels (figure S11); and second, on the basis that in historically mining-affected catchments the modelled 100-year flood extent closely delineates the limit of metal and metalloid concentrations above DIL and soil remediation guidelines *(85, 86)* (figure S12). River lengths and floodplain areas contaminated per catchment were added to calculate regional and global totals (table S14). Finally, an assessment of global contamination hazard was determined by calculating the number of people/livestock living on contaminated floodplains impacted by metal mining activity and/or TDFs (tables S16-17).

For the global impacts modelling, contaminated areas mapped in catchments were reprojected to the Mollweide equal area projection at 500 m resolution and merged to create global spatial layers. These were spatially overlaid on gridded human population (GPW), livestock (GLW3), and irrigated areas (GMIA), which were also re-projected by nearest neighbor to Mollweide equal area projection resampled to 500 m.

<u>Validation of WAPHA process-based model of sediment-associated mining contaminant dispersal in river systems</u>

Using river sediment samples collected and geochemically analyzed by some of the authors (MGM, PAB, GB) over the last 20 years *(6, 8, 12, 16-18, 20, 21, 32, 50-54, 56-61, 64, 73, 85, 86)*, we have undertaken extensive ground-truthing and field-based validation of our sediment-associated mining contaminant dispersal model (see above) and the multi-scalar maps of metal mining affected river channels and floodplains generated (see tables S8-S11). Geochemical data from channel bed and overbank sediment (<0.063 mm) collected at 344 sites have been used from 15 river catchments in Bulgaria, England, Romania and Wales, which range in size from 46 km^2 to 232,193 km^2. We tested model predictions against field measurements for Pb (164 channel bed and 174 overbank sites), Zn (164 channel bed and 158 overbank sites), Cu (170 channel bed sites) and As (159 channel bed sites) over a river network length of c. 1,110 km. As our primary aim was to establish whether or not our model correctly identified contaminated river reaches downstream of a metal mine, model predictions were compared to field geochemical data using Dutch intervention limits *(87)*. If the model correctly predicted that elemental concentrations were at or above the DIL target soil remediation intervention limit, this was classified as a 'hit'. If the model predicted that a site was contaminated (i.e., metal or As concentrations at or above the intervention limit) but field measurements showed that metal and As values fell between DIL and target soil remediation limits, this was classified as a 'near-miss', as the site had potentially harmful element concentrations above those that would be considered desirable for ecosystem and human health. Last, where model predictions did not match geochemical field data three sub-categories of 'miss' were recognized: 1. model predicted contamination, but the site was not contaminated (false positive); 2. model predicted no contamination, but the site is contaminated and is located within a floodplain reach (false negative). This is likely the result of the remobilization of contaminated floodplain sediment, most usually related to historical metal mining activities in a catchment *(21, 50)*. 3. model predicted no contamination, but the site is contaminated and is not located within a floodplain reach (false negative). This exercise demonstrated good model performance and predictions most notably for Pb (overall 69% 'hits', 18% 'near-misses' and 13% 'misses'), followed by Cu (overall 59% 'hits', 29% 'near-misses' and 12% 'misses'), Zn (overall 55% 'hits', 32% 'near-misses' and 13% 'misses') and As (overall 55% 'hits', 6% 'near-misses' and 39% 'misses').

Using the Socioeconomic Data and Applications Center (NASA-SEDAC) population data of the year 2020 (*33*), and FAO Gridded Livestock of the World database (GLW v3.1) (*34*), the number of people and livestock (cattle, goat, and sheep) living on mining-affected floodplains was determined (tables S12-S14). The area of irrigated land based on FAO Global Map of Irrigation Areas (GMIA) in mining impacted floodplains was also calculated (table S15). Our geospatial integration of metal mine, tailings storage facilities, tailings dam failures, hydrographic, geomorphic, demographic and livestock databases enable us to evaluate globally the likely population exposure and uptake of contaminant metals into the human food chain (table S15).

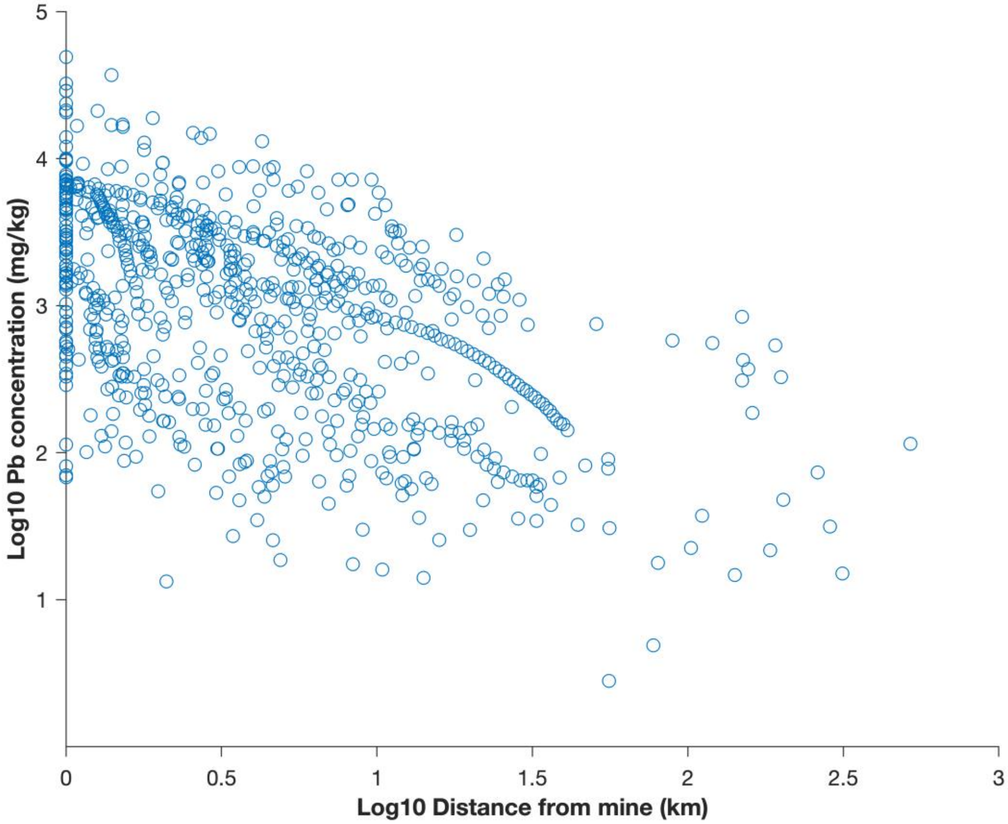

Figure S1. Log_{10} Pb concentrations against log_{10} distances downstream of individual mine sites (n=79 mine sites).

280

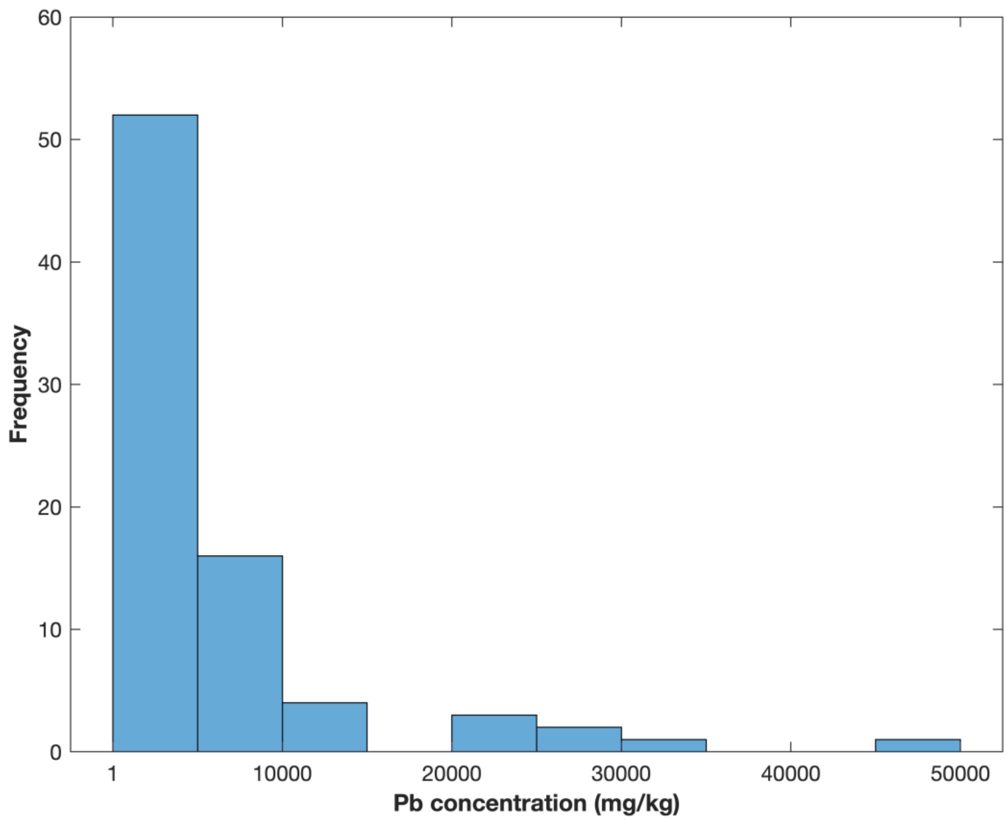

Figure S2. Frequency distribution of observed Pb concentrations at mine sites reported (n=79 mine sites).

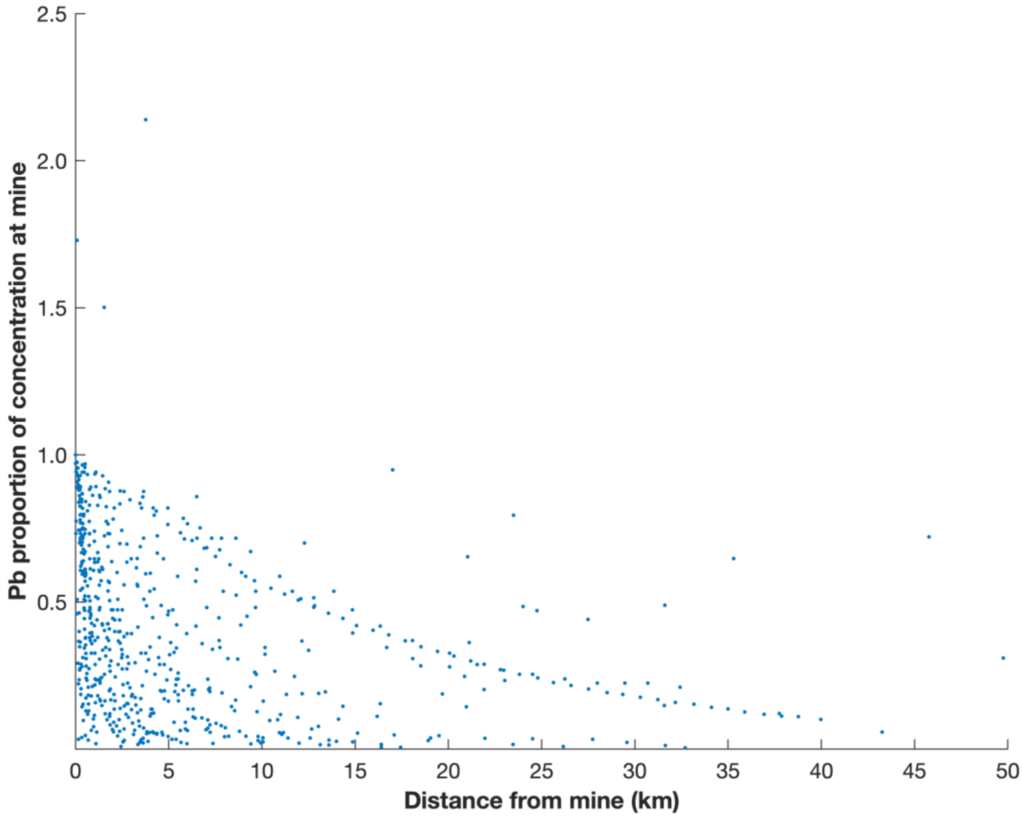

Figure S3. Pb proportions from source mines by distance (n=79 mine sites).

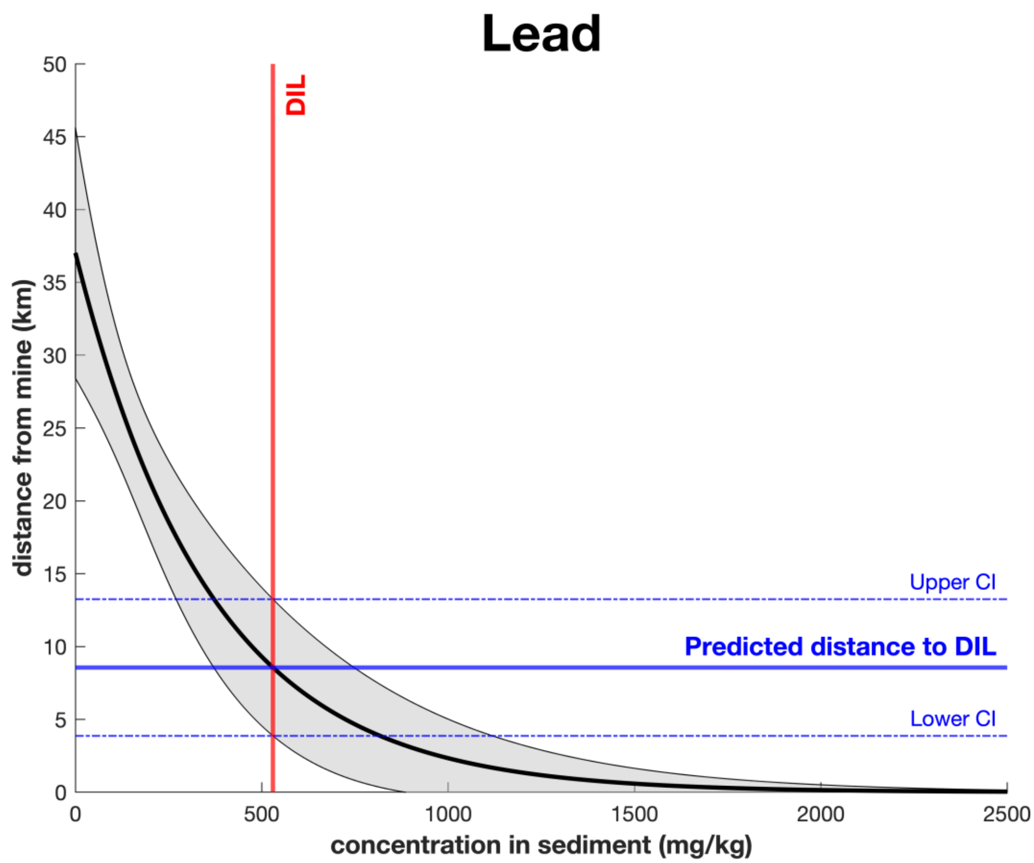

Figure S4. Predicted distance against Pb values. Predicted curve in solid black with grey shading to 95% confidence intervals. The Dutch Intervention Limit (DIL) of 530 mg/kg is given as a vertical reference line (solid red), with predicted attenuation distance from mine (solid blue line), with upper and lower 95% confidence intervals (dashed blue lines).

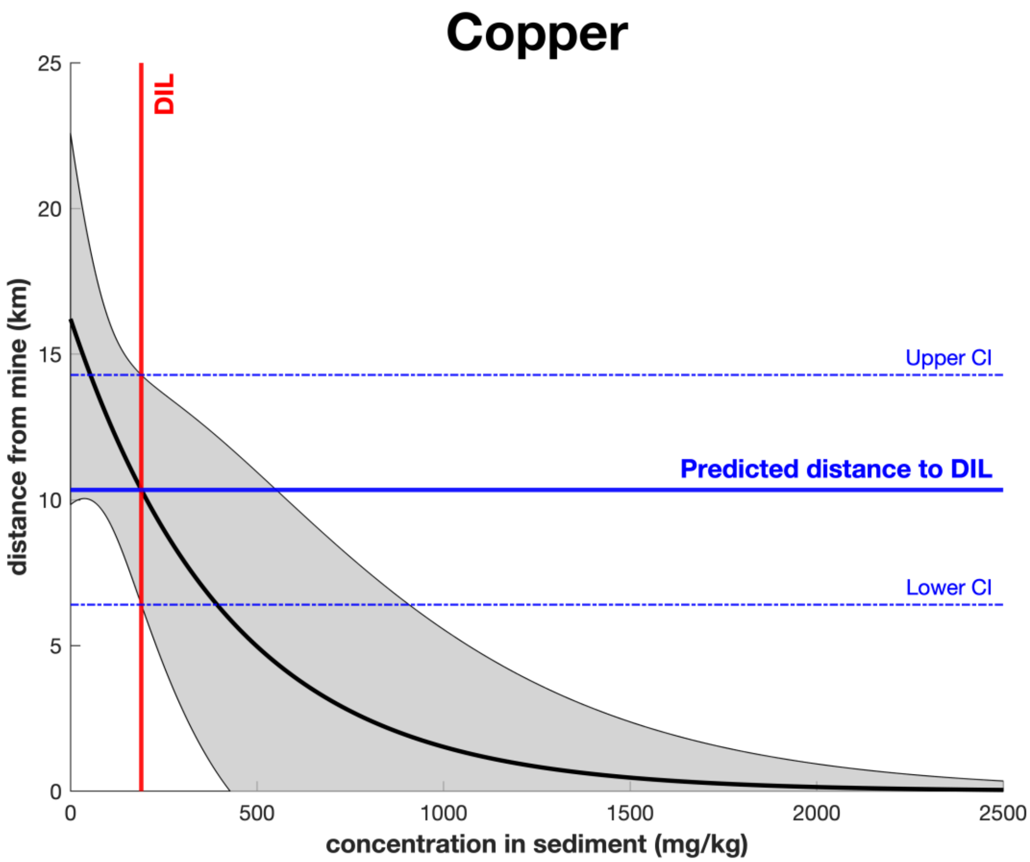

Figure S5. Predicted distance against Cu values. Predicted curve in solid black with grey shading to 95% confidence intervals. The Dutch Intervention Limit (DIL) of 190 mg/kg is given as a vertical reference line (solid red), with predicted attenuation distance from mine (solid blue line), with upper and lower 95% confidence intervals (dashed blue lines).

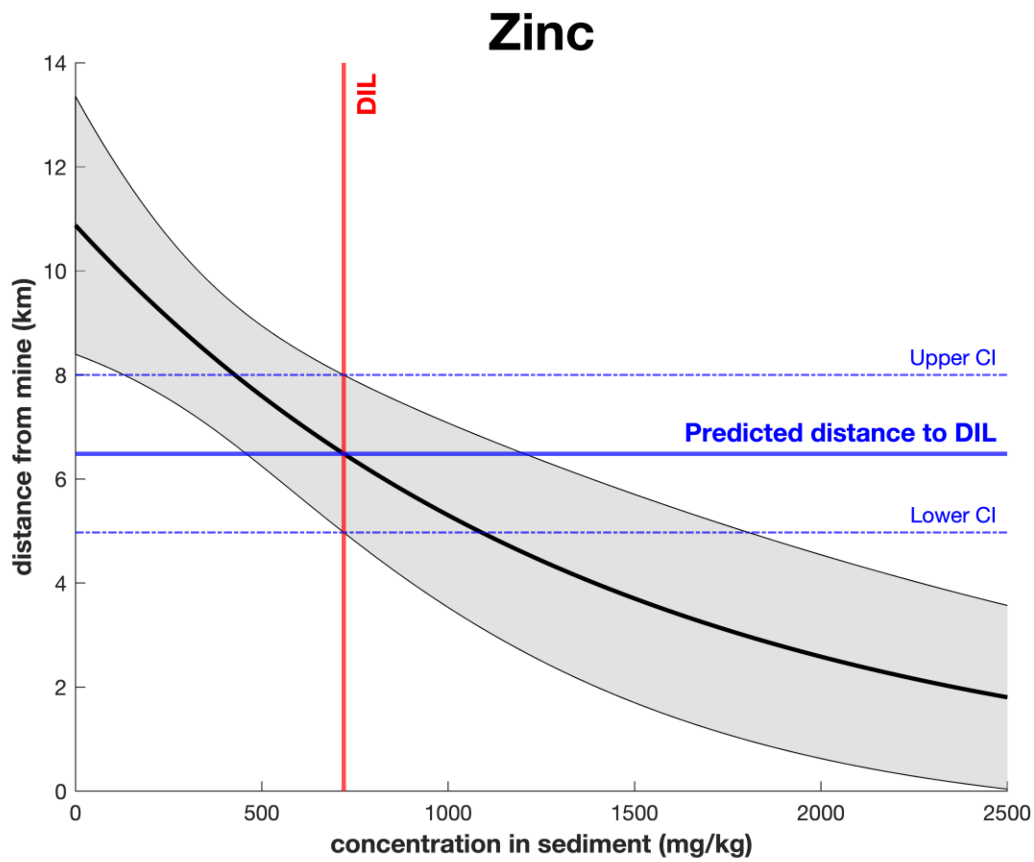

Figure S6. Predicted distance against Zn values. Predicted curve in solid black with grey shading to 95% confidence intervals. The Dutch Intervention Limit (DIL) of 720 mg/kg is given as a vertical reference line (solid red), with predicted attenuation distance from mine (solid blue line), with upper and lower 95% confidence intervals (dashed blue lines).

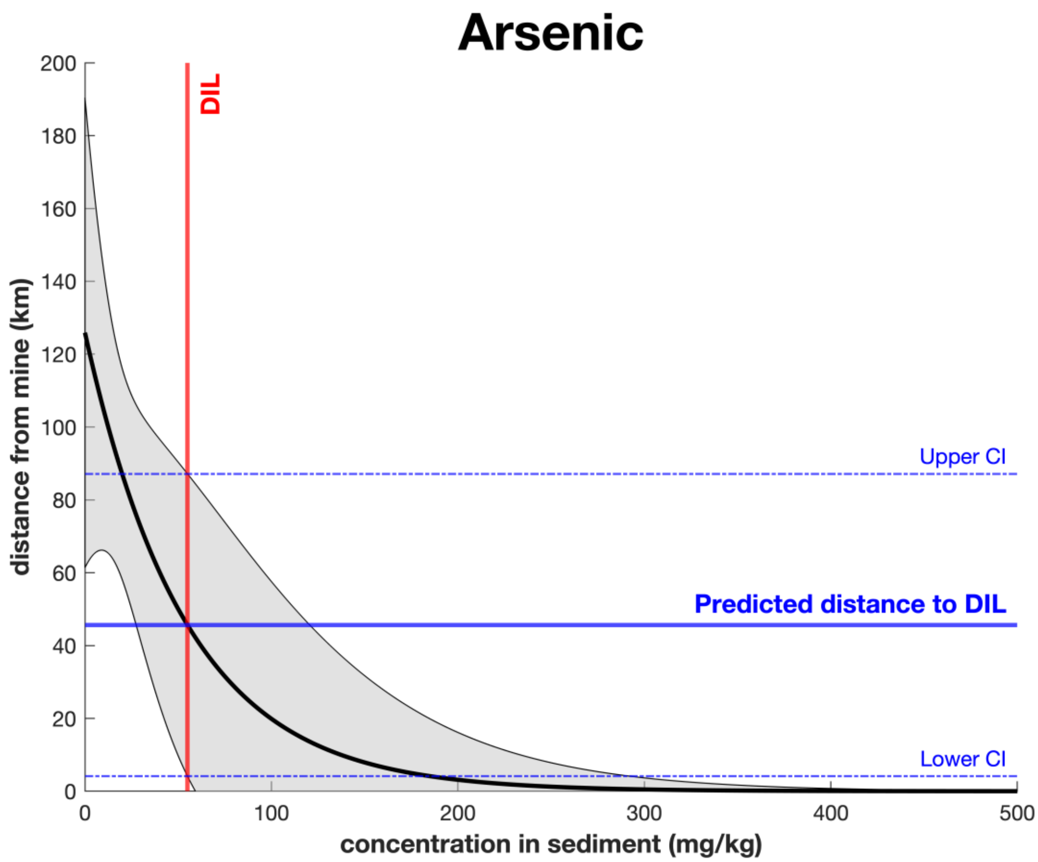

Figure S7. Predicted distance against As values. Predicted curve in solid black with grey shading to 90% confidence intervals. The Dutch Intervention Limit (DIL) of 55 mg/kg is given as a vertical reference line (solid red), with predicted attenuation distance from mine (solid blue line), with upper and lower 90% confidence intervals (dashed blue lines).

330

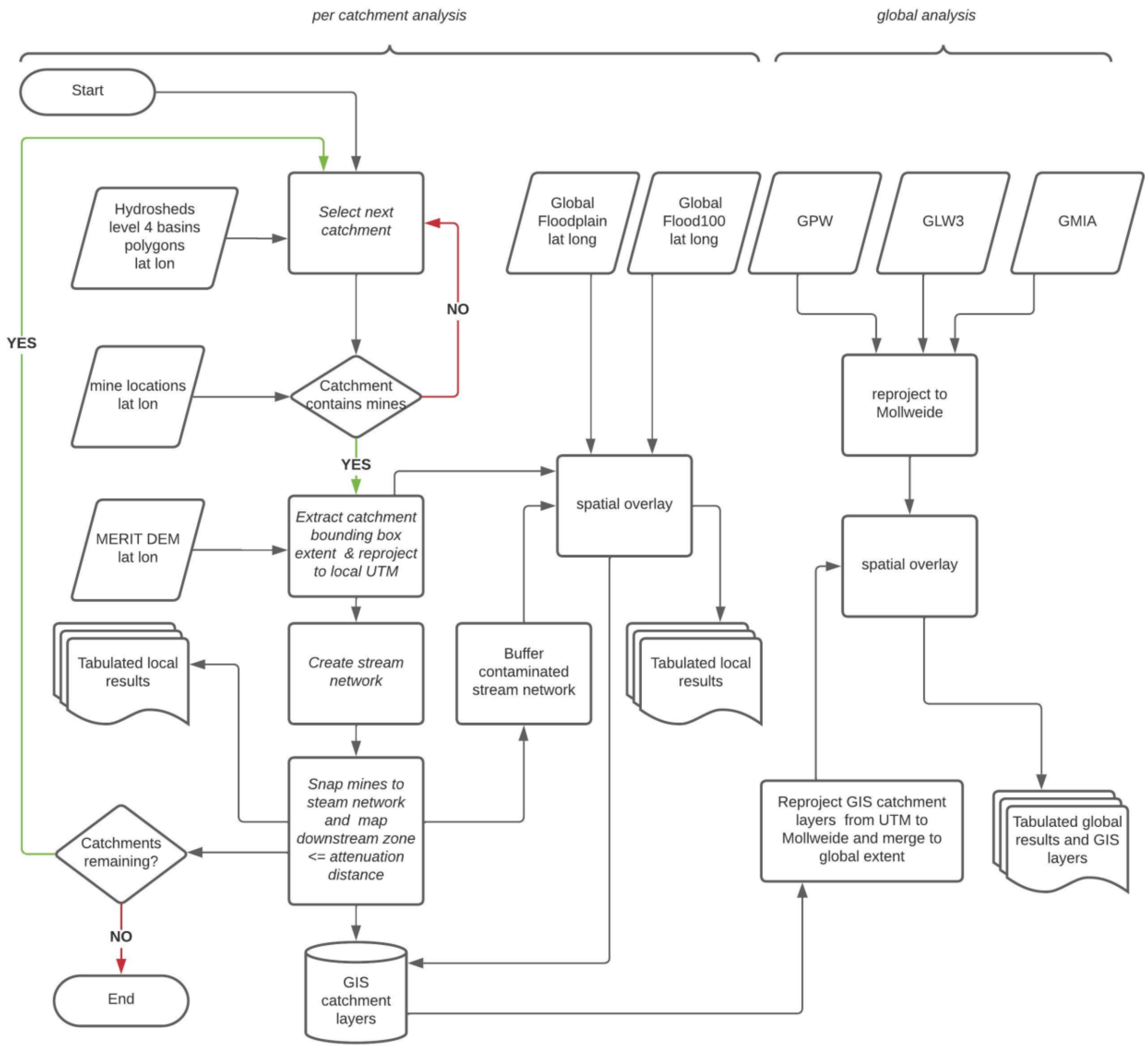

Figure S8. Modelling workflow.

a)

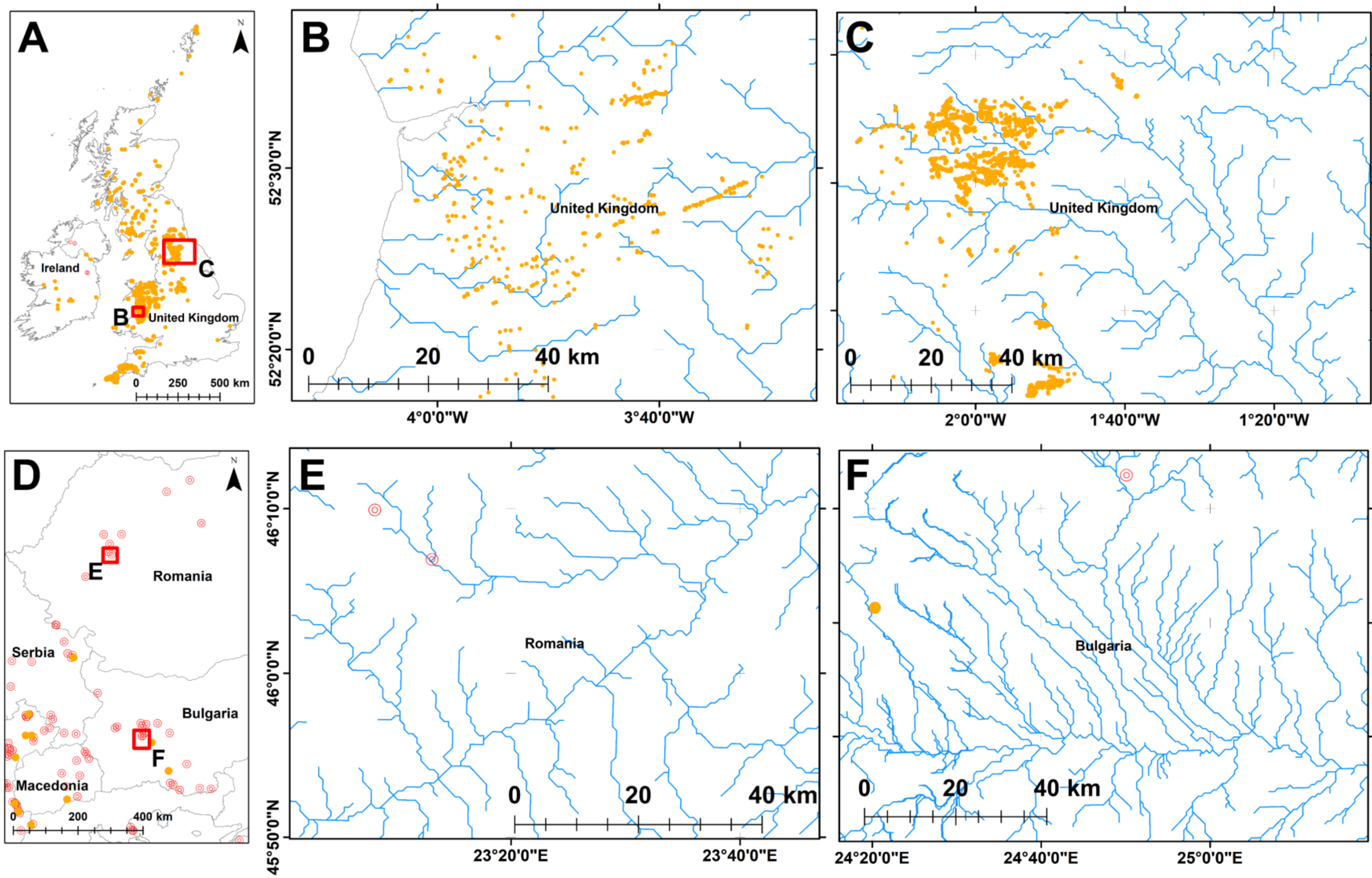
A
Ireland
C
B
United Kingdom
0
250
500 km
B
52°30'0"N
52°20'0"N
United Kingdom
0
20
40 km
4°0'0"W
3°40'0"W
C
54°30'0"N
54°20'0"N
54°10'0"N
United Kingdom
0
20
40 km
2°0'0"W
1°40'0"W
1°20'0"W
D
Romania
E
Serbia
Bulgaria
F
Macedonia
0
200
400 km
E
46°10'0"N
46°0'0"N
45°50'0"N
Romania
0
20
40 km
23°20'0"E
23°40'0"E
F
42°30'0"N
42°20'0"N
42°10'0"N
Bulgaria
0
20
40 km
24°20'0"E
24°40'0"E
25°0'0"E

b)

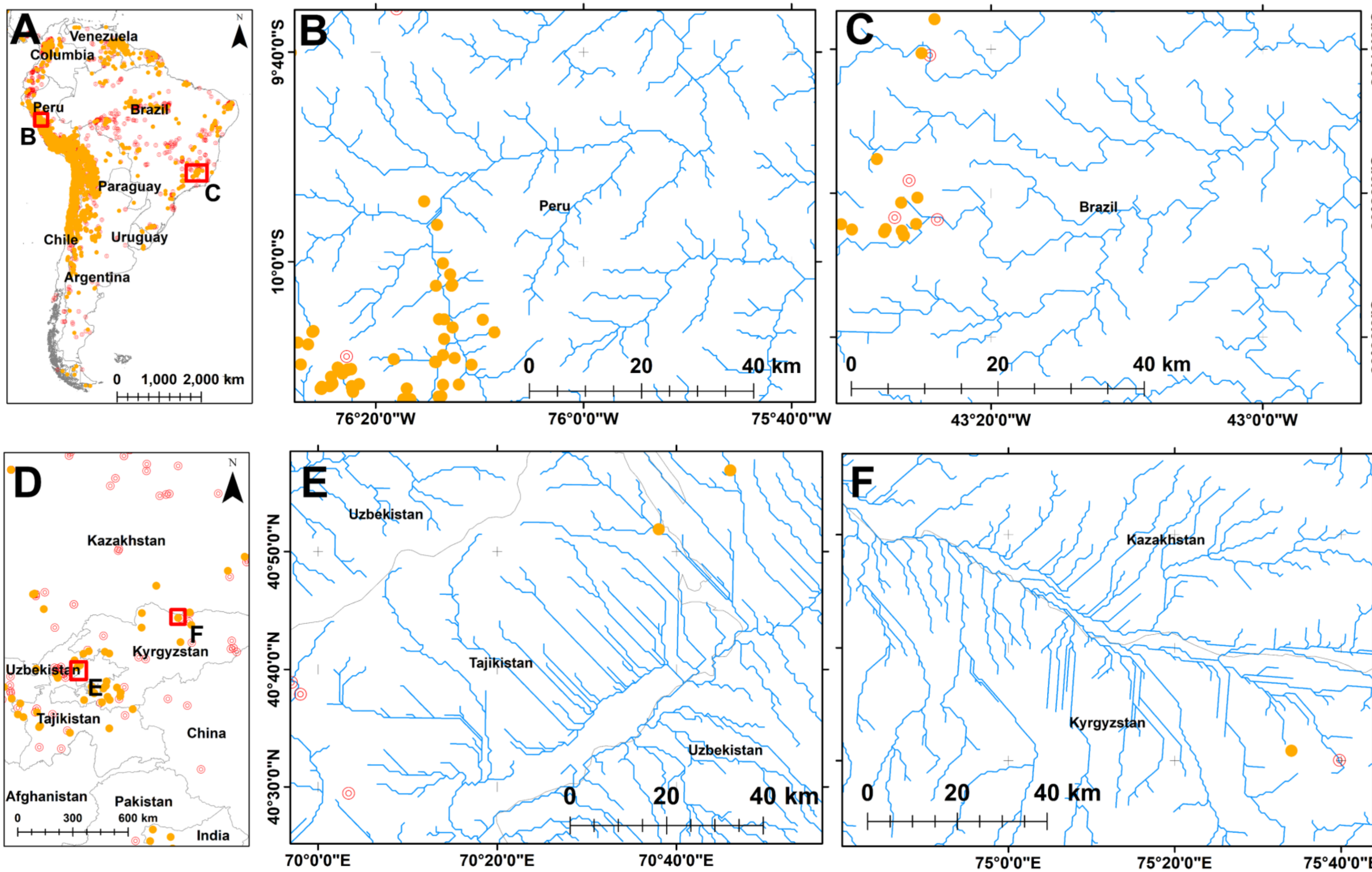
A
Venezuela
Columbia
Peru
Brazil
B
Paraguay
C
Chile
Uruguay
Argentina
0 1,000 2,000 km
N
B
9°40'0"S
10°0'0"S
Peru
0 20 40 km
76°20'0"W
76°0'0"W
75°40'0"W
C
20°10'0"S
20°20'0"S
20°30'0"S
Brazil
0 20 40 km
43°20'0"W
43°0'0"W
D
N
Kazakhstan
F
Kyrgyzstan
Uzbekistan
E
Tajikistan
China
Afghanistan
Pakistan
0 300 600 km
India
E
Uzbekistan
40°50'0"N
40°40'0"N
40°30'0"N
Tajikistan
Uzbekistan
0 20 40 km
70°0'0"E
70°20'0"E
70°40'0"E
F
Kazakhstan
43°0'0"N
42°50'0"N
42°40'0"N
Kyrgyzstan
0 20 40 km
75°0'0"E
75°20'0"E
75°40'0"E

337
338

Map symbols		Modelled contamination
Inactive metal mine	National Border	Contamination extent to the distance given by lower confidence interval (CI)
Active metal mine	GFPLAIN250 floodplain	Additional contamination beyond the lower CI extending to the predicted distance
Stream network	100-year flood limit	Additional contamination beyond the predicted distance extending to the upper CI

Figure S9. Inactive and active mines and modelled stream network in example a) UK and Eastern European, and b) South American/Central Asian catchments. Figure S9a: B) Rheidol and Ystwyth Rivers, mid-Wales, C) River Swale, northern England; E) Romania, and F) Bulgaria. A) and D) show regional index maps for the UK and Eastern European sites, respectively.

Figure S9b: B) Peru, C) Brazil; E) Turkmenistan and Uzbekistan, and F) Kazakhstan and Kyrgyzstan. A) and D) show regional index maps for the South American and Central Asian sites, respectively.

a)

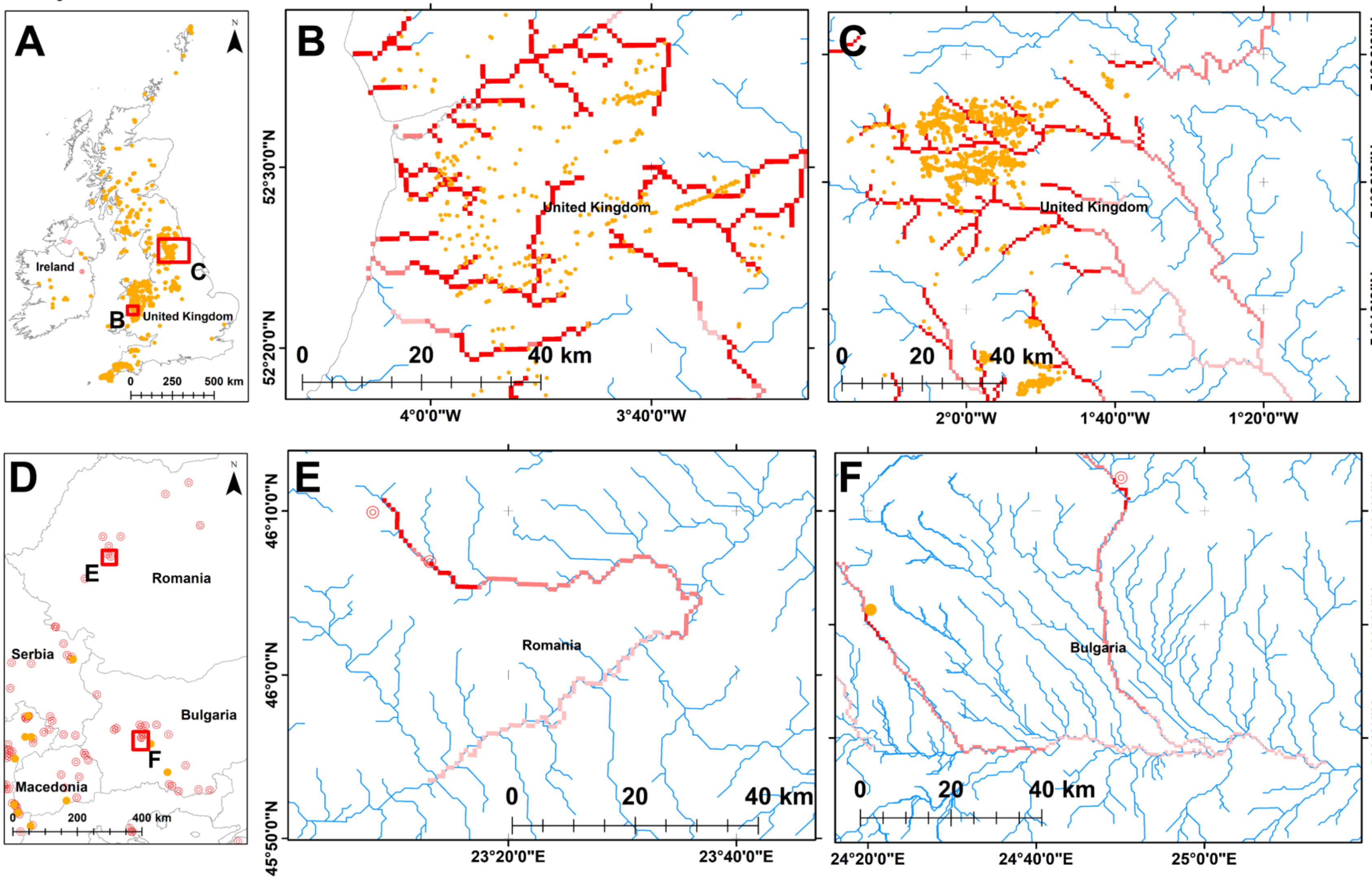
A
Ireland
C
B
United Kingdom
0 250 500 km
B
52°30'0"N
52°20'0"N
United Kingdom
0 20 40 km
4°0'0"W
3°40'0"W
C
United Kingdom
0 20 40 km
2°0'0"W
1°40'0"W
1°20'0"W
54°30'0"N
54°20'0"N
54°10'0"N
D
E
Romania
Serbia
Bulgaria
F
Macedonia
0 200 400 km
E
46°10'0"N
46°0'0"N
45°50'0"N
Romania
0 20 40 km
23°20'0"E
23°40'0"E
F
Bulgaria
0 20 40 km
24°20'0"E
24°40'0"E
25°0'0"E
42°30'0"N
42°20'0"N
42°10'0"N

347
348

b)

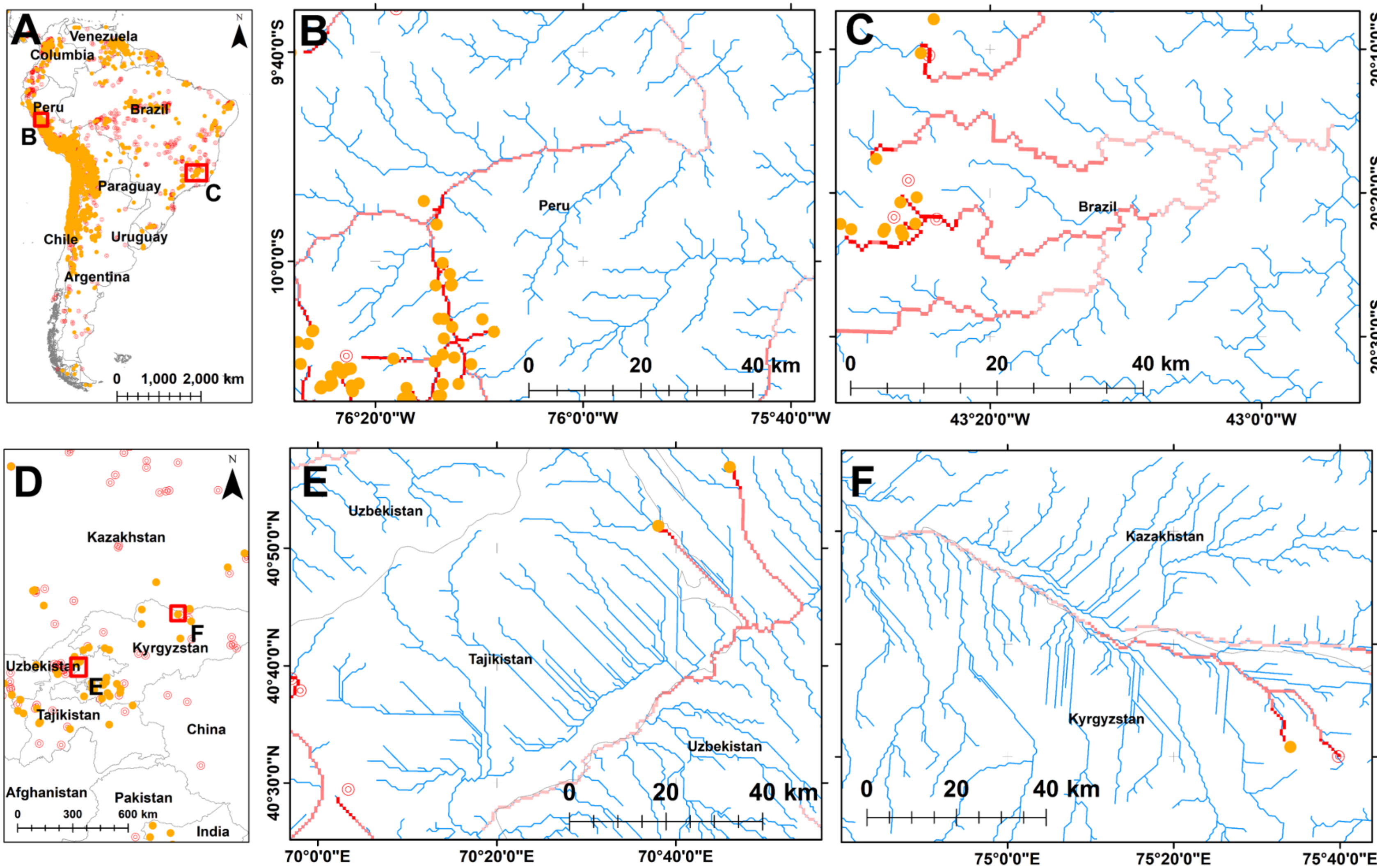
A
Venezuela
Columbia
Peru
Brazil
B
Paraguay
C
Chile
Uruguay
Argentina
0 1,000 2,000 km
B
9°40'0"S
10°0'0"S
Peru
0 20 40 km
76°20'0"W
76°0'0"W
75°40'0"W
C
20°10'0"S
20°20'0"S
20°30'0"S
Brazil
0 20 40 km
43°20'0"W
43°0'0"W
D
Kazakhstan
F
Kyrgyzstan
Uzbekistan
E
Tajikistan
China
Afghanistan
Pakistan
India
0 300 600 km
E
Uzbekistan
Tajikistan
Uzbekistan
40°50'0"N
40°40'0"N
40°30'0"N
0 20 40 km
70°0'0"E
70°20'0"E
70°40'0"E
F
Kazakhstan
Kyrgyzstan
43°0'0"N
42°50'0"N
42°40'0"N
0 20 40 km
75°0'0"E
75°20'0"E
75°40'0"E

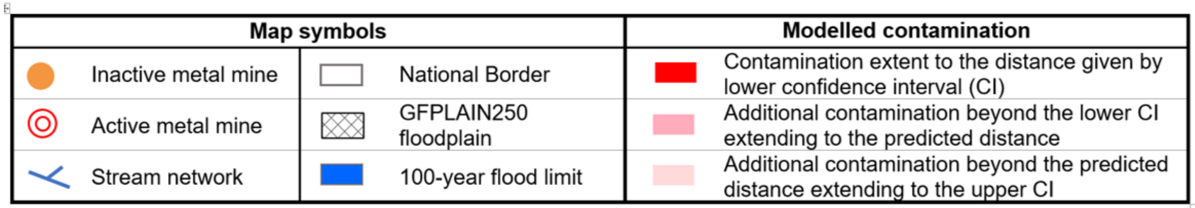

Figure S10. Examples of contaminated river channel reaches linked to inactive and active mines in the modelled stream network in a) UK and Eastern European, and b) South American/Central Asian catchments.

Figure S10a. B) Rheidol and Ystwyth Rivers, mid-Wales, C) River Swale, northern England; E) Romania, and F) Bulgaria. A) and D) show regional index maps for the UK and Eastern European sites, respectively.

Figure S10b. B) Peru, C) Brazil; E) Turkmenistan and Uzbekistan, and F) Kazakhstan and Kyrgyzstan. A) and D) show regional index maps for the South American and Central Asian sites, respectively.

a)

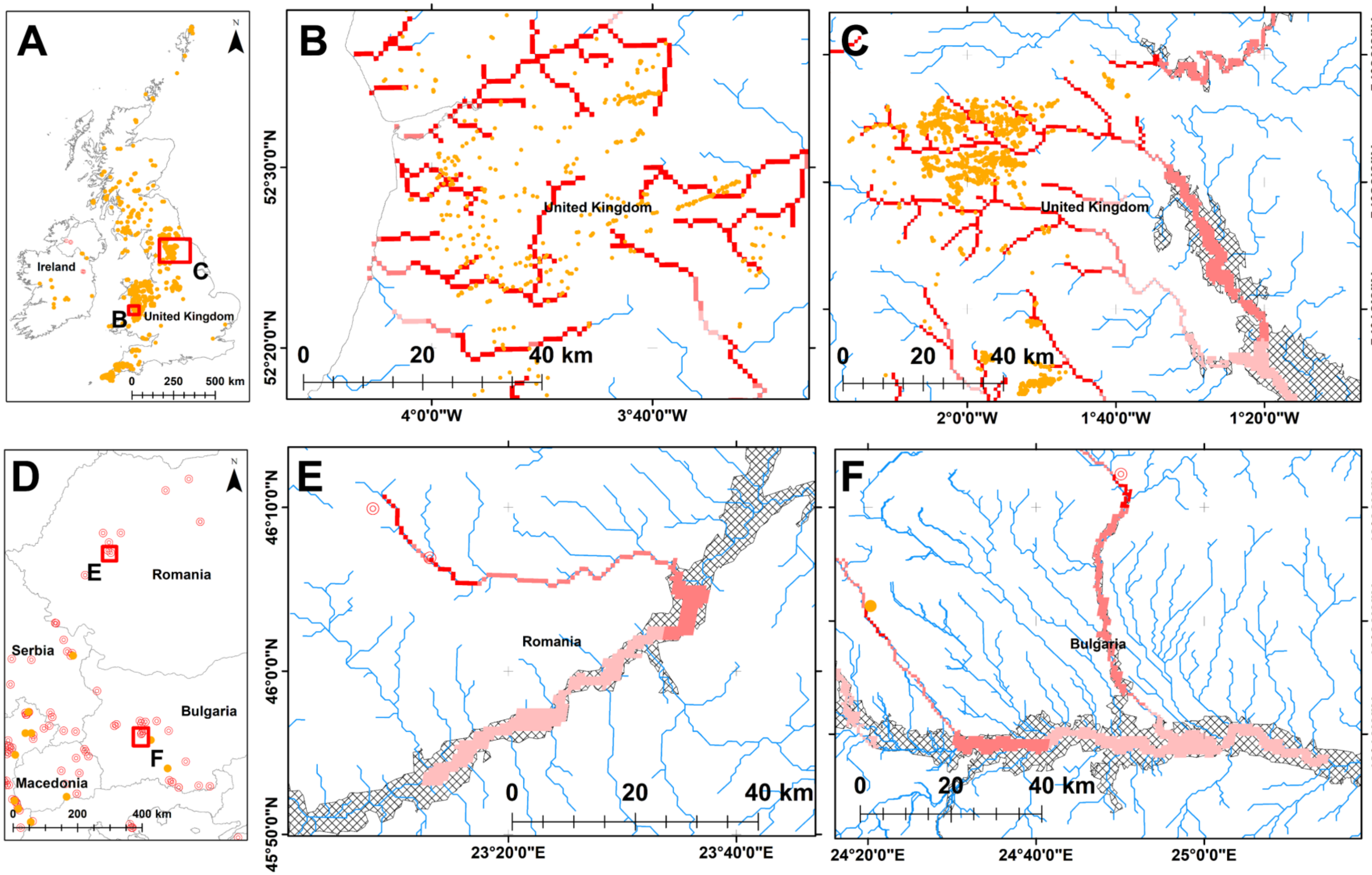

A
Ireland
United Kingdom
B
C
0 250 500 km
B
United Kingdom
0 20 40 km
52°30'0"N
52°20'0"N
4°0'0"W
3°40'0"W
C
United Kingdom
0 20 40 km
54°30'0"N
54°20'0"N
54°10'0"N
2°0'0"W
1°40'0"W
1°20'0"W
D
Romania
E
Serbia
Bulgaria
F
Macedonia
0 200 400 km
E
Romania
0 20 40 km
46°10'0"N
46°0'0"N
45°50'0"N
23°20'0"E
23°40'0"E
F
Bulgaria
0 20 40 km
42°30'0"N
42°20'0"N
42°10'0"N
24°20'0"E
24°40'0"E
25°0'0"E

b)

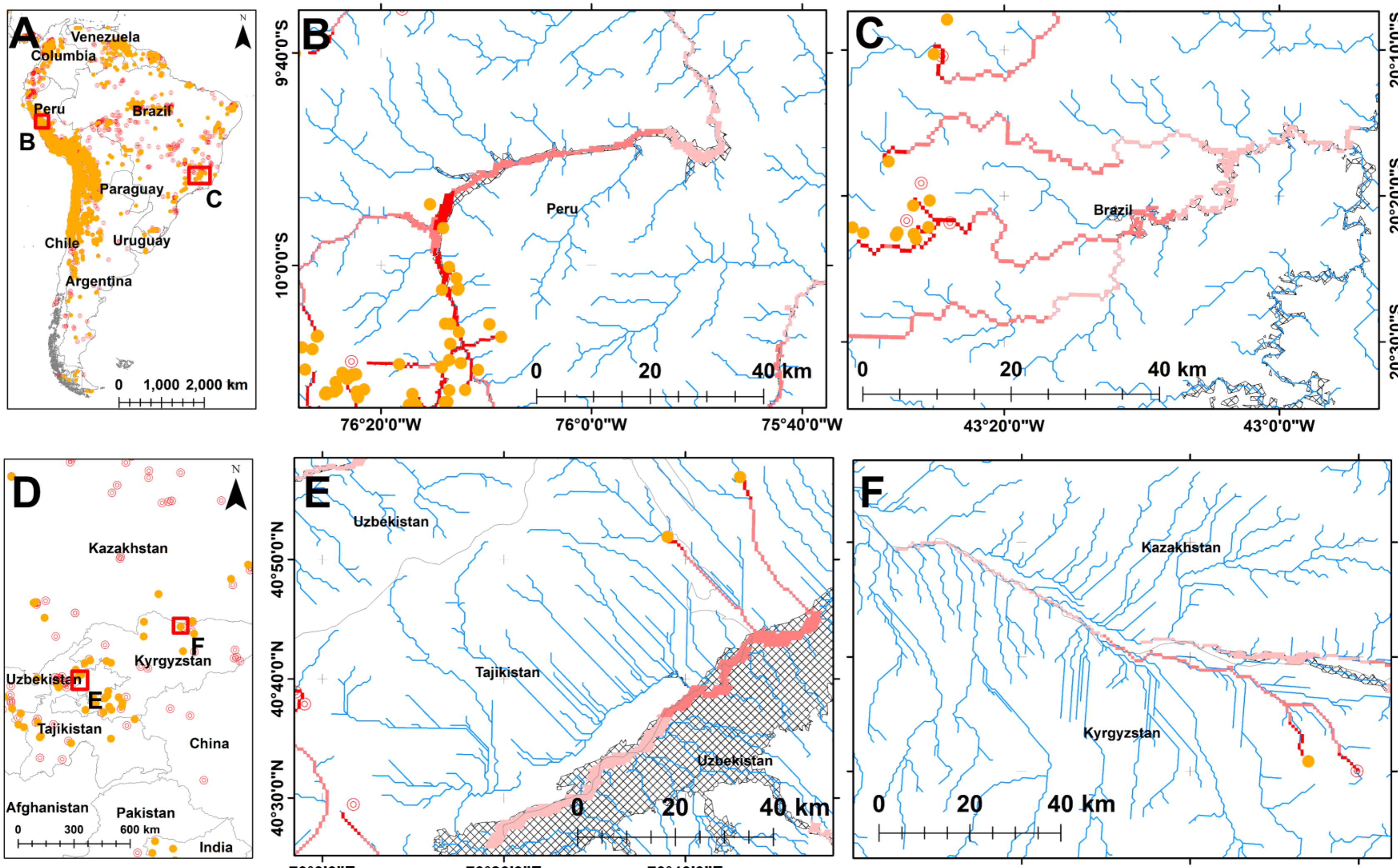

A
Venezuela
Columbia
Peru
Brazil
B
Paraguay
C
Chile
Uruguay
Argentina
0 1,000 2,000 km
B
Peru
9°40'0"S
10°0'0"S
0 20 40 km
76°20'0"W
76°0'0"W
75°40'0"W
C
Brazil
20°10'0"S
20°20'0"S
20°30'0"S
0 20 40 km
43°20'0"W
43°0'0"W
D
Kazakhstan
F
Kyrgyzstan
Uzbekistan
E
Tajikistan
China
Afghanistan
Pakistan
India
0 300 600 km
E
Uzbekistan
Tajikistan
Uzbekistan
40°50'0"N
40°40'0"N
40°30'0"N
0 20 40 km
70°0'0"E
70°20'0"E
70°40'0"E
F
Kazakhstan
Kyrgyzstan
43°0'0"N
42°50'0"N
42°40'0"N
0 20 40 km
75°0'0"E
75°20'0"E
75°40'0"E

362
363

Map symbols		Modelled contamination
Inactive metal mine	National Border	Contamination extent to the distance given by lower confidence interval (CI)
Active metal mine	GFPLAIN250 floodplain	Additional contamination beyond the lower CI extending to the predicted distance
Stream network	100-year flood limit	Additional contamination beyond the predicted distance extending to the upper CI

Figure S11. Examples of contaminated floodplains and river channel reaches linked to inactive and active mines in the modelled stream network in a) UK and Eastern European, and b) South American/Central Asian catchments.

Figure S11a. B) Rheidol and Ystwyth Rivers, mid-Wales, C) River Swale, northern England; E) Romania, and F) Bulgaria. A) and D) show regional index maps for the UK and Eastern European sites, respectively.

Figure S11b. B) Peru, C) Brazil; E) Turkmenistan and Uzbekistan, and F) Kazakhstan and Kyrgyzstan. A) and D) show regional index maps for the South American and Central Asian sites, respectively.

a)

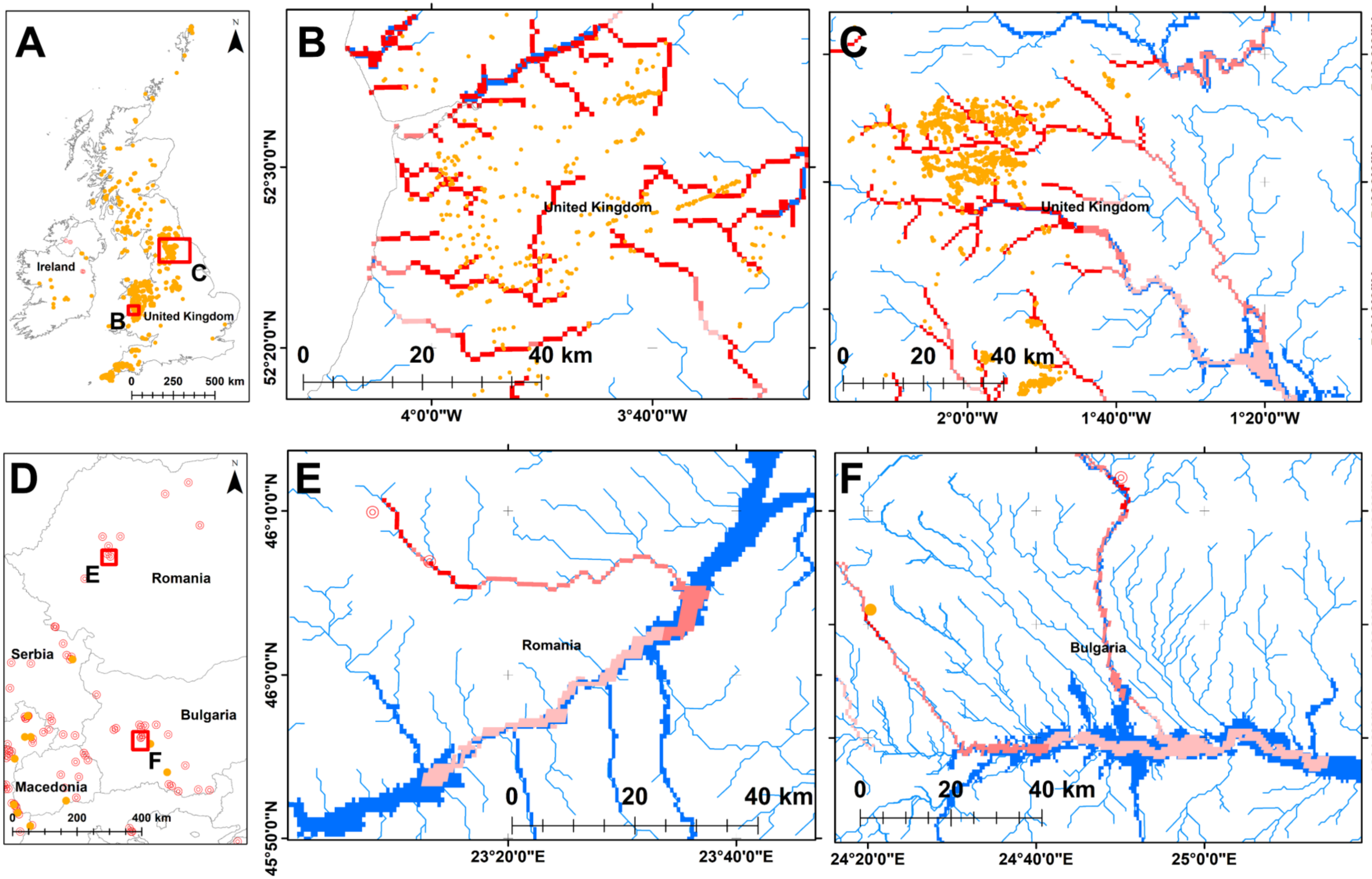
A
Ireland
C
B
United Kingdom
0 250 500 km
B
United Kingdom
0 20 40 km
52°30'0"N
52°20'0"N
4°0'0"W
3°40'0"W
C
United Kingdom
0 20 40 km
54°30'0"N
54°20'0"N
54°10'0"N
2°0'0"W
1°40'0"W
1°20'0"W
D
E
Romania
Serbia
Bulgaria
F
Macedonia
0 200 400 km
E
Romania
0 20 40 km
46°10'0"N
46°0'0"N
45°50'0"N
23°20'0"E
23°40'0"E
F
Bulgaria
0 20 40 km
42°30'0"N
42°20'0"N
42°10'0"N
24°20'0"E
24°40'0"E
25°0'0"E

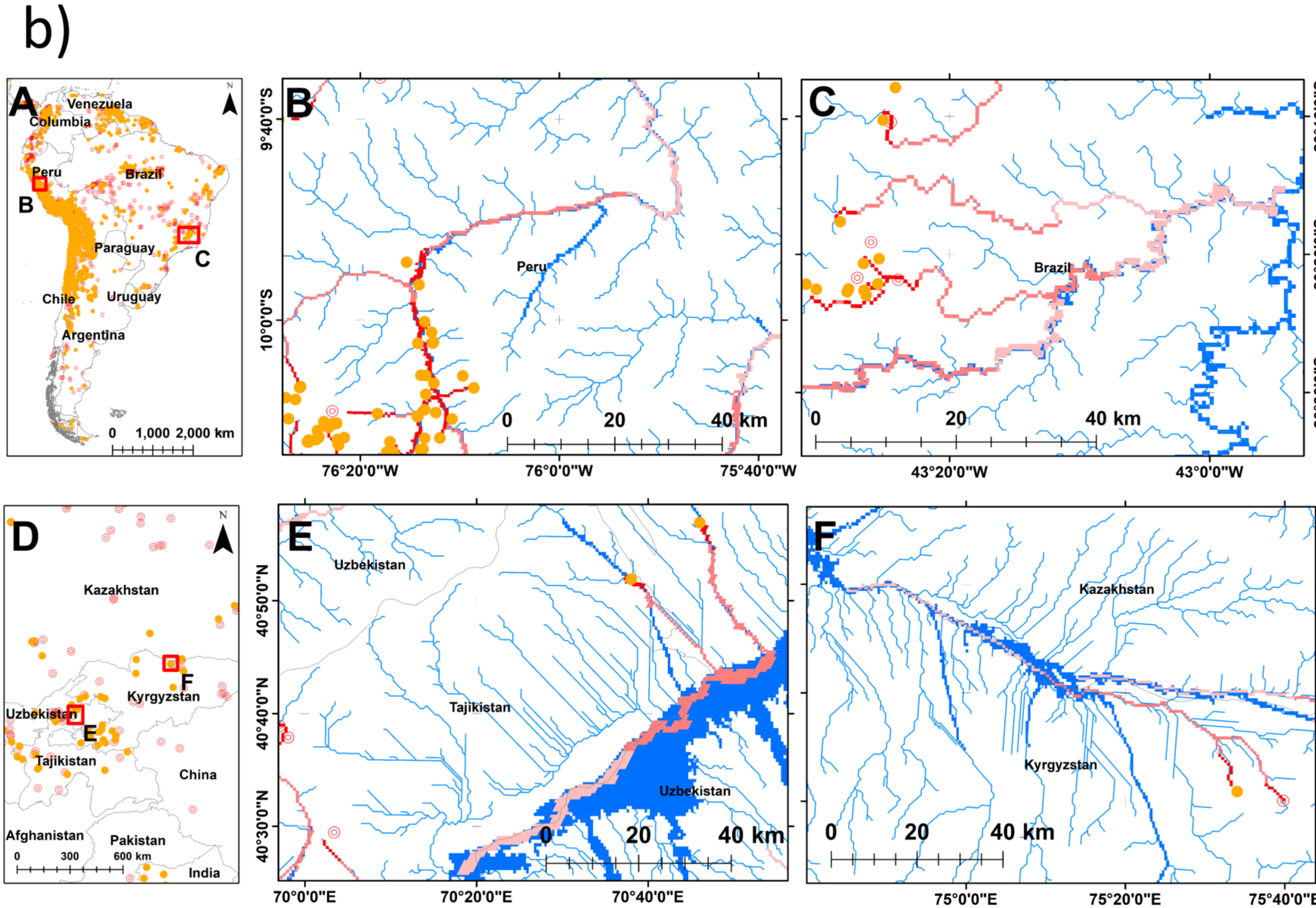
b)
A
Venezuela
Columbia
Peru
Brazil
B
Paraguay
C
Chile
Uruguay
Argentina
0 1,000 2,000 km
B
Peru
9°40'0"S
10°0'0"S
0 20 40 km
76°20'0"W
76°0'0"W
75°40'0"W
C
Brazil
20°10'0"S
20°20'0"S
20°30'0"S
0 20 40 km
43°20'0"W
43°0'0"W
D
Kazakhstan
F
Kyrgyzstan
Uzbekistan
E
Tajikistan
China
Afghanistan
Pakistan
India
0 300 600 km
E
Uzbekistan
Tajikistan
Uzbekistan
40°50'0"N
40°40'0"N
40°30'0"N
0 20 40 km
70°0'0"E
70°20'0"E
70°40'0"E
F
Kazakhstan
Kyrgyzstan
43°0'0"N
42°50'0"N
42°40'0"N
0 20 40 km
75°0'0"E
75°20'0"E
75°40'0"E

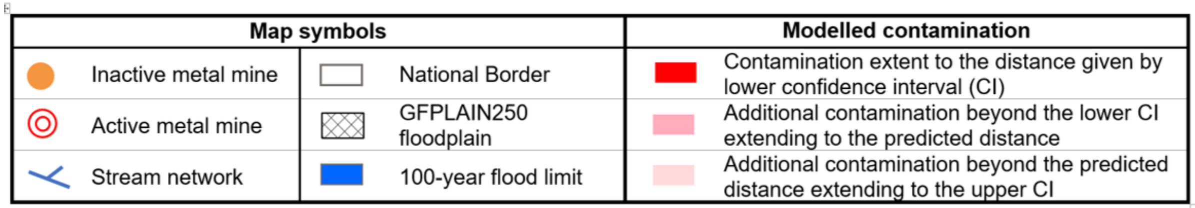

Figure S12. Examples of contaminated reaches and areas subject to 100-year R I floods linked to inactive and active mines in the modelled stream network in: a) UK and Eastern European, and b) South American/Central Asian catchments.
Figure S12a. B) Rheidol and Ystwyth Rivers, mid-Wales, C) River Swale, northern England; E) Romania, and F) Bulgaria. A) and D) show regional index maps for the UK and Eastern European sites, respectively.
Figure S12b. B) Peru, C) Brazil; E) Turkmenistan and Uzbekistan, and F) Kazakhstan and Kyrgyzstan. A) and D) show regional index maps for the South American and Central Asian sites, respectively.

	Total	N. America	S. America	Africa	Asia	Europe	Oceania
INACTIVE							
S&P	811	282	92	97	189	56	95
WAPHA	159,735	80,995	14,577	377	1,473	9,080	53,233
ACTIVE							
S&P	1773	209	183	172	978	112	119
WAPHA	22,609	11,871	3,240	1,227	1,817	1,024	3,430

Table S1. The total number of metal mines in the S&P Global Market Intelligence database and the WAPHA database for inactive and recently operating mines by continent.

Country	Source
Burkina Faso, Ghana, Mali, South Africa and Tanzania	Ashton et al. (2001) (*88*) Lourens and Water (2016) (*89*) Chuhan-Pole et al. (2017) (*90*)
Argentina	Delloite (*91*)
Australia	Australian Mines Atlas (*92*) Werner et al. (2020) (*93*)
Belgium	Government of The Wallonia-Brussels Federation (*94*)
Brazil	Sonter et al. (2017) (*95*) Mindat.org (*96*) National Mining Agency (ANM) Brazil (*97*)
Bulgaria	Bird et al. (2010 a, b) (*35, 51*) Gold mining and processing in Bulgaria (March 2010) (*98*)
Canada	Geological Survey of Canada (*99*) Ontario Prospectors Association (*100*)
China	Wei and Yang (2010) (*101*) Li et al. (2014) (*102*) Chen et al. (2015) (*103*) Chen et al., (2016) (*104*) Zhang et al. (2012) (*105*)
Columbia	Pinedo-Hernández et al. (2015) (*106*)
Cuba	CIA (1977) (*107*)
Czech Republic	Štrupl et al. (2017) (*108*)
Finland	Räisänen et al. (2013) (*109*)
France	Nasri et al. (2020) (*110*)
Germany	Federal Institute for Geosciences and Natural Resources (BGR) (*111*)
Hungary	Mining and Geological Survey of Hungary (*112*)
India	Ministry of Mines, Government of India (*113*)
Ireland	Environmental Protection Agency (EPA), Ireland (*114*)
Italy	Institute for the Protection and Environmental Research, Italy (*115*)
Kazakhstan	Mining, Development and Environment in Central Asia: Toolkit Companion with Case Studies (*116*) Central Asian Countries Geoportal (*117*)
Kyrgyz Republic	Mining, Development and Environment in Central Asia: Toolkit Companion with Case Studies (*116*) Central Asian Countries Geoportal (*117*)
Laos	Kyophilvong (2009) (*118*)
Mexico	University of Texas (*119*) Geo-Mexico (*120*)
Myanmar	Gardiner et al. (2014) (*121*) Gardiner et al. (2015) (*122*)
Netherlands	Leenaers (1989) (*84*)
Paraguay	Eckel et al. (1959) (*123*)
Peru	PwC (2020) (*124*) Van Geen et al. (2012) (*125*)
Portugal	LNEG (2000) (*126*)
Romania	European Commission (2017) (*127*)
Russia	Walker et al. (2003) (*128*) Jarsjö et al. (2017) (*129*)

Country	Source
Serbia	Monthel et al. (2002) (*130*) Atanacković et al. (2016) (*131*)
Slovakia	Ministry of Environment of the Slovak Republic (*132*)
Slovenia	Gosar et al. (2014) (*133*)
Tajikistan	Central Asian Countries Geoportal (*117*)
Thailand	Assawincharoenkij et al. (2018) (*134*) Li et al. (2017) (*135*)
UK	Potter & Johnston (2014) (*136*) European Commission (2017) (*127*) BritPits (*25*)
Venezuela	Santos-Frances et al. (2011) (*137*) Schruben et al. (1997) (*138*) Veiga et al. (2006) (*139*)
USA	U. S. Government open data portal (*140*) Mineral Resources Data System (MRDS) (*24*)
Tailings Storage Facilities	Bowker and Chambers (2015) (*141*) Concha Larrauri and Lall (2018) (*32*) WISE Uranium Project (*28*) Global Tailings Portal (*29*) Li et al (2020) (*142*) Tang et al. (2020) (*143*)

Table S2. List of data sources used for compiling the global metal mining and tailings storage facilities database

MINES		Total	Antimony	Arsenic	Barium	Cadmium	Caesium	Chromium	Cobalt	Copper	Gold
INACTIVE											
Africa	S&P	97	0	0	0	0	0	0	1	17	65
	WAPHA	377	1	2	3	1	0	34	8	51	124
Asia	S&P	189	1	0	0	0	0	0	0	45	88
	WAPHA	1473	71	10	8	2	0	26	16	264	272
Australia	S&P	95	0	0	0	0	0	0	0	7	78
	WAPHA	53233	304	247	157	0	0	209	36	6287	38947
Europe	S&P	56	0	0	0	0	0	0	0	11	12
	WAPHA	9080	14	38	140	3	0	71	19	1108	152
North America	S&P	282	0	0	0	0	0	0	1	35	176
	WAPHA	80995	1063	606	1785	82	7	1421	225	11962	29006
South America	S&P	92	0	0	0	0	0	0	0	16	51
	WAPHA	14577	135	45	47	4	0	19	42	2678	1852
ACTIVE											
Africa	S&P	172	0	0	0	0	0	1	3	41	97
	WAPHA	1227	8	5	29	4	1	104	38	194	372
Asia	S&P	978	3	0	0	0	0	0	0	229	446
	WAPHA	1817	25	2	25	10	0	26	18	361	612
Australia	S&P	119	0	0	0	0	0	0	0	18	74
	WAPHA	3430	15	3	6	4	1	16	14	192	2734
Europe	S&P	112	0	0	0	0	0	0	0	45	41
	WAPHA	1024	12	19	37	15	0	97	20	223	125
North America	S&P	209	3	0	0	0	0	0	0	43	111

MINES			Total	Antimony	Arsenic	Barium	Cadmium	Caesium	Chromium	Cobalt	Copper	Gold
	WAPHA		11871	207	148	243	29	0	471	47	1375	3977
South America	S&P		183	0	0	0	0	0	0	0	64	72
	WAPHA		3240	94	28	41	25	0	22	10	706	923

Table S3a. The total number of metal mines in the S&P Global Market Intelligence database and the WAPHA database for inactive and active mines by commodity, and the number of mines from S&P already recorded in WAPHA database (Antimony to Gold).

MINES		Total	Lead	Lithium	Mercury	Nickel	Platinum	Silver	Thallium	Tin	Tungsten	Uranium	Witherite	Zinc
INACTIVE														
Africa	S&P	97	1	0	0	3	3	0	0	1	0	0	0	6
	WAPHA	377	25	1	1	9	67	14	0	10	5	6	0	15
Asia	S&P	189	13	0	0	14	0	1	0	4	0	0	0	23
	WAPHA	1473	99	0	144	21	342	19	0	88	56	2	0	33
Australia	S&P	95	1	0	0	3	0	1	0	2	0	0	0	3
	WAPHA	53233	1596	13	29	321	75	635	0	3233	612	92	0	440
Europe	S&P	56	1	0	0	17	0	0	0	3	0	0	0	12
	WAPHA	9080	6360	0	9	38	38	135	0	705	20	1	68	161
North America	S&P	282	5	0	0	8	1	31	0	0	0	0	0	25
	WAPHA	80995	11831	72	1150	145	392	11158	1	227	0	4714	2116	3032
South America	S&P	92	1	0	0	4	0	6	0	5	0	0	0	9
	WAPHA	14577	8293	10	32	17	12	709	0	248	157	47	0	230
ACTIVE														
Africa	S&P	172	2	0	0	4	11	2	0	3	1	0	0	7
	WAPHA	1227	56	11	2	29	153	95	0	49	8	49	0	20
Asia	S&P	978	27	0	0	84	4	11	0	8	15	0	0	151
	WAPHA	1817	124	2	11	85	66	40	0	150	62	2	0	196
Australia	S&P	119	2	0	0	11	0	2	0	1	1	0	0	10
	WAPHA	3430	38	29	1	114	36	49	0	44	15	30	0	89
Europe	S&P	112	4	0	0	6	1	2	0	0	4	0	0	9
	WAPHA	1024	165	2	11	48	23	56	0	9	30	10	0	122
North America	S&P	209	1	0	0	8	0	25	0	0	0	0	0	18

MINES		Total	Lead	Lithium	Mercury	Nickel	Platinum	Silver	Thallium	Tin	Tungsten	Uranium	Witherite	Zinc
	WAPHA	11871	1005	33	212	128	165	1558	0	32	0	1398	365	478
South America	S&P	183	2	0	0	7	0	10	0	7	1	0	0	20
	WAPHA	3240	341	9	18	18	33	361	0	293	131	9	0	178

Table S3b. The total number of metal mines in the S&P Global Market Intelligence database and the WAPHA database for inactive and active mines by commodity, and the number of mines from S&P already recorded in WAPHA database (Lead to Zinc)

	N. Amer	S. Amer	Asia	Africa	Europe	Oceania	Total (Global)
TDF	107	58	47	11	25	9	257
TSF	1365	1865	5512	336	1932	577	11,587
Total	1472	1923	5559	347	1957	586	11,844

Table S4. Number of currently intact tailings storage facilities (TSF) and number of tailings dam failures (TDF).

	Total	N. America	S. America	Asia	Africa	Europe	Oceania
GTP	1919	526	423	281	327	54	308
WAPHA	11,585	1365	1865	5512	336	1932	575

Table S5. Tailings storage facilities in the Global Tailings Portal (GTP) and the WAPHA database by continent.

Metal/	**DIL (mg/kg)**	**Predicted DIL distance (km)**	**95% CI (±km)**	**F (df reg, df res)**	**p**	**RMSE**
Lead	530	8.56	4.69	73.9 (2,737)	<0.001	32.6
Copper	190	10.34	3.94	26.5(2,249)	<0.001	25.1
Zinc	720	6.49	1.51	71.0(2,704)	<0.001	15.9
Metalloid	**DIL (mg/kg)**	**Predicted DIL distance (km)**	**90% CI (±km)**	**F (df reg, df res)**	**p**	**RMSE**
Arsenic	55	45.63	41.52	13.2 (2,38)	<0.001	83.7

Table S6. Dutch Intervention Limit (DIL) threshold distance estimates from source mines by negative exponential regression of observed concentrations. RMSE = root mean squared error.

Mined mineral commodity	Associated elements
Antimony	As
Arsenic	As
Barium	Pb
Cadmium	Zn
Cobalt	Cu
Copper	Cu and As
Gold	As
Lead	Pb and Cu
Mercury	As and Pb
Nickel	Cu
Platinum	Cu
Silver	As and Pb
Thallium	As and Pb
Tin	As and Pb
Tungsten	As and Pb
Uranium	As and Pb
Witherite	Pb
Zinc	Zn and Pb

Table S7. Elements used to select the attenuation rates to model downstream contamination associated with mines based on the main mineral commodities produced

435

Sediment type	Country	River basin	Basin area (km^2)	Year of field-work	Number of sample points	Hit (%) Conc. ≥ Dutch intervention value (530 mg/kg)	Near-miss (%) Conc. ≥ Dutch target remediation value (85 mg/kg)	Miss (%)		
								1	2	3
Overall						69	18	1	9	3
Channel (<0.063 mm)	England	Swale	1,446	2000	34	71	6	3	15	6
	England	Swale	1,446	2001	26	73	15	4		8
	England	Swale	1,446	2002	25	84	8			8
	Wales	Severn	11,420	2000	15	27	60	13		
	Wales	Ystwyth	194	2012	23	70			30	
	Wales	Rheidol	189	2012	19	95	5			
	Wales	Leri	66	2012	16	44	56			
	Wales	Clarach	46	2012	6	100				
Overbank (<0.063 mm)	England	Swale	1,446	2000	34	65	12		18	6
	England	Swale	1,446	2001	34	62	21		15	3
	England	Swale	1,446	2002	35	60	17		17	6
	England	Swale	1,446	2006	33	100				
	England	Wharfe	900	2006	11	91	9			
	Wales	Severn	11,420	2006	27	37	56	4	4	

Table S8. Pb Ground-truthing of model outputs (*8*, *16*, *18*, *20*, *21*, *50*, *61*, *85*, *86*)

Sediment type	Country	River basin	Basin area (km^2)	Year of field-work	Number of sample points	Hit (%) Conc. ≥ Dutch intervention value (720 mg/kg)	Near-miss (%) Conc. ≥ Dutch target remediation value (140 mg/kg)	Miss (%)		
								1	2	3
Overall						55	32	5	6	2
Channel (<0.063 mm)	England	Swale	1,446	2000	34	76	6		15	3
	England	Swale	1,446	2001	26	85	12		4	
	England	Swale	1,446	2002	25	80	12		8	
	Wales	Severn	11,420	2000	15	20	67	13		
	Wales	Ystwyth	194	2012	23	61	39			
	Wales	Rheidol	189	2012	19	21	79			
	Wales	Leri	66	2012	16		56	44		
	Wales	Clarach	46	2012	6		100			
Overbank (<0.063 mm)	England	Swale	1,446	2000	34	71	9		15	6
	England	Swale	1,446	2001	34	76	15		6	3
	England	Swale	1,446	2002	35	69	11		14	6
	England	Swale	1,446	2006	17	24	76			
	England	Wharfe	900	2006	11		100			
	Wales	Severn	11,420	2006	27	41	33	26		

Table S9. Zn Ground-truthing of model outputs (*8*, *16*, *18*, *20*, *21*, *50*, *61*, *85*, *86*)

Sediment type	Country	River basin	Basin area (km^2)	Year of field-work	Number of sample points	Hit (%) Conc. ≥ Dutch intervention value (190 mg/kg)	Near-miss (%) Conc. ≥ Dutch target remediation value (36 mg/kg)	Miss (%)		
								1	**2**	**3**
Overall						59	29	4	7	1
Channel (<0.063 mm)	Romania	Danube	232,193	2009	12	100				
	Romania	Aries	3,005	2004	17	76	18	6		
	Romania	Aries	3,005	2002	20	35	35		30	
	Romania	Mures	30,332	2002	15	73	27			
	Bulgaria	Danube	47,413	2004	22	91			9	
	Bulgaria	Maritsa	35,086	2005	29	62	17	7	3	10
	Bulgaria	Arda	5,213	2005	19	21	58	16	5	
	Bulgaria	Iskur	8,646	2004	23	52	39		9	
	Bulgaria	Timok	4,626	2004	1	100				
	Bulgaria	Ogosta	3,157	2004	12	17	83			

Table S10. Cu Ground-truthing of model outputs (*21*, *32*, *51-53*, *56-58*, *73*)

Sediment type	Country	River basin	Basin area (km^2)	Year of field-work	Number of sample points	Hit (%) Conc. ≥ Dutch intervention value (55 mg/kg)	Near-miss (%) Conc. ≥ Dutch target remediation value (29 mg/kg)	Miss (%)		
								1	**2**	**3**
Overall						55	6	36	3	
Channel (<0.063 mm)	Romania	Danube	232,193	2009	12	100				
	Romania	Aries	3,005	2004	17	29	18	53		
	Romania	Aries	3,005	2002	20	35	5	60		
	Romania	Mures	30,332	2002	15	67		33		
	Bulgaria	Danube	47,413	2004	22	95			5	
	Bulgaria	Maritsa	35,086	2005	29	45	10	38	7	
	Bulgaria	Arda	5,213	2005	19	11	11	74	5	
	Bulgaria	Iskur	8,646	2004	12	58		42		
	Bulgaria	Timok	4,626	2004	1		100			
	Bulgaria	Ogosta	3,157	2004	12	95			5	

Table S11. As Ground-truthing of model outputs (*21*, *32*, *51-53*, *56-58*, *73*)

	Country	95th percentile (1000s of people)	50th percentile (1000s of people)	5th percentile (1000s of people)
GLOBAL		39325	23478	4527
Asia		25300	14527	2661
	China	16959	9742	1950
	Japan	1848	884	20
	India	1431	593	30
	South Korea	1204	794	300
	Philippines	918	791	101
	Thailand	586	355	18
	Malaysia	358	298	70
	Uzbekistan	336	82	3
	Indonesia	258	121	0
	Turkey	213	141	25
	Laos	187	107	5
	Tajikistan	151	105	16
	Vietnam	149	60	2
	North Korea	148	136	9
	Taiwan	143	143	78
	Myanmar	115	69	11
	Iran	112	40	7
	Kyrgyzstan	48	12	0
	Armenia	40	11	2
	Cambodia	36	11	0
	Kazakhstan	30	19	11
	Pakistan	8	3	1
	Jordan	6	4	0
	Azerbaijan	5	3	0
	Palestine	4	0	0
	Georgia	3	3	0
	Israel	1	0	0
	Mongolia	1	0	0
	Afghanistan	0	0	0
	Oman	0	0	0
N. America		6043	4088	942

	Country	95th percentile (1000s of people)	50th percentile (1000s of people)	5th percentile (1000s of people)
	United States (south of 60º N)	4444	3172	793
	Mexico	846	461	80
	Canada (south of 60º N)	279	188	58
	Honduras	184	90	2
	Dominican Republic	81	58	4
	El Salvador	60	33	0
	Guatemala	48	30	2
	Nicaragua	43	29	2
	Panama	32	14	1
	Haiti	17	7	0
	Cuba	7	3	0
	Costa Rica	2	2	0
	Puerto Rico	0	0	0
S. America		2288	1527	306
	Brazil	916	674	105
	Colombia	415	177	16
	Peru	267	185	66
	Chile	257	230	75
	Bolivia	208	159	36
	Ecuador	117	44	1
	Argentina	63	28	4
	Venezuela	27	17	2
	French Guiana	9	9	1
	Guyana	7	3	0
	Uruguay	1	1	0
	Suriname	1	0	0
Europe		3249	1727	423
	Germany	765	348	76
	United Kingdom	557	312	53
	Spain	327	282	57
	France	281	100	36
	Poland	238	58	18
	Belgium	183	127	27

	Country	95th percentile (1000s of people)	50th percentile (1000s of people)	5th percentile (1000s of people)
	Russia (south of 60º N)	130	83	24
	Bulgaria	128	60	23
	Italy	107	84	20
	Slovakia	84	16	1
	Serbia	70	31	19
	Romania	64	28	1
	Austria	59	29	18
	Ireland	51	34	13
	Portugal	51	42	0
	Czech Republic	34	14	1
	Ukraine	31	24	21
	Albania	25	24	4
	Hungary	10	0	0
	Bosnia and Herzegovina	10	5	2
	Croatia	9	8	7
	Macedonia	9	3	1
	Greece	5	1	1
	Montenegro	0	0	0
	Kosovo	17	10	3
	Northern Cyprus	4	2	0
Oceania		532	421	69
	Australia	505	408	68
	Papua New Guinea	18	8	1
	New Zealand	9	6	0
Africa		1913	1188	126
	Democratic Republic of the Congo	238	168	17
	Algeria	224	89	12
	Rwanda	222	170	6
	South Africa	195	138	24
	Ghana	157	91	3
	Burkina Faso	131	70	4
	Morocco	106	52	25
	Zambia	99	89	3

	Country	95th percentile (1000s of people)	50th percentile (1000s of people)	5th percentile (1000s of people)
	Uganda	85	57	7
	Zimbabwe	79	55	8
	Tanzania	77	48	7
	Tunisia	43	41	4
	Côte d'Ivoire	42	21	3
	Mali	33	17	2
	Guinea	30	17	1
	Nigeria	23	7	0
	Burundi	20	0	0
	Ethiopia	18	9	0
	Eritrea	11	4	0
	Liberia	11	9	0
	Niger	11	4	0
	Gabon	11	4	0
	Sudan	9	8	0
	Sierra Leone	8	3	0
	Senegal	8	5	0
	Swaziland	8	4	0
	Kenya	6	3	0
	Mozambique	5	2	0
	Botswana	3	2	0
	Angola	0	0	0
	Namibia	0	0	0
	Republic of Congo	0	0	0
	Malawi	0	0	0
	Mauritania	0	0	0

Table S12: Impact of metal mining: Populations in contaminated floodplains. Areas of contaminated floodplains from active and inactive mines were estimated by the WAPHA model (95th, 50th and 5th percentile confidence intervals) and overlaid with GPWv4 gridded population to estimate population living in contaminated floodplains to the nearest 1000 people. Countries are listed by continent in descending order of populations affected with continental total rows shaded grey. Excludes territories with no floodplains mapped by GFPLAIN250.

Rank	Country	Continent	95^{th} percentile (1000s of people)	50^{th} percentile (1000s of people)	5^{th} percentile (1000s of people)
1	China	Asia	16959	9742	1950
2	United States (south of 60° N)	N. America	4444	3172	793
3	Japan	Asia	1848	884	20
4	South Korea	Asia	1204	794	300
5	Philippines	Asia	918	791	101
6	Brazil	S. America	916	674	105
7	India	Asia	1431	593	30
8	Mexico	N. America	846	461	80
9	Australia	Oceania	505	408	68
10	Thailand	Asia	586	355	18
11	Germany	Europe	765	348	76
12	United Kingdom	Europe	557	312	53
13	Malaysia	Asia	358	298	70
14	Spain	Europe	327	282	57
15	Chile	S. America	257	230	75
16	Canada (south of 60° N)	N. America	279	188	58
17	Peru	S. America	267	185	66
18	Colombia	S. America	415	177	16
19	Rwanda	Africa	222	170	6
20	Democratic Republic Congo	Africa	238	168	17

Table S13: Impact of metal mining: Top 20 country populations living in contaminated floodplains. Areas of contaminated floodplains from active and inactive mines were estimated by the WAPHA model (95^{th}, 50^{th} and 5^{th} percentile confidence intervals) and overlaid with GPWv4 gridded population to estimate population living in contaminated floodplains to the nearest 1000 people. Countries are listed in descending order of populations affected. Excludes territories with no floodplains mapped by GFPLAIN250. Data derived from table S12.

	Country	95th percentile (1000s of people)	50th percentile (1000s of people)	5th percentile (1000s of people)
GLOBAL		20685	11394	1244
Asia		11619	5716	538
	China	7034	3507	323
	Japan	1447	541	12
	India	946	377	11
	South Korea	705	553	155
	Thailand	405	240	9
	Uzbekistan	293	71	2
	Malaysia	145	120	1
	Tajikistan	121	101	16
	Laos	111	74	1
	Iran	87	25	2
	Myanmar	67	23	1
	Philippines	65	21	0
	Armenia	35	6	1
	Vietnam	34	12	1
	Cambodia	31	10	0
	North Korea	28	12	2
	Kyrgyzstan	19	9	0
	Turkey	15	5	0
	Kazakhstan	10	3	0
	Jordan	6	4	0
	Pakistan	5	0	0
	Indonesia	4	2	0
	Palestine	4	0	0
	Georgia	1	1	0
	Israel	1	0	0
	Oman	0	0	0
	Mongolia	0	0	0
Northern America		5103	3411	467
	United States (south of 60º N)	3888	2719	425
	Mexico	617	349	16
	Canada (south of 60º N)	188	114	22

	Country	95th percentile (1000s of people)	50th percentile (1000s of people)	5th percentile (1000s of people)
	Honduras	154	83	2
	Dominican Republic	80	51	0
	El Salvador	60	32	0
	Nicaragua	42	27	1
	Guatemala	28	18	1
	Panama	23	5	1
	Haiti	16	7	0
	Cuba	7	3	0
South America		1571	932	113
	Brazil	561	316	67
	Colombia	359	129	5
	Chile	226	205	13
	Bolivia	185	137	12
	Peru	150	104	13
	Argentina	33	14	1
	Ecuador	20	6	0
	Venezuela	19	14	1
	French Guiana	9	3	1
	Guyana	7	3	0
	Uruguay	1	1	0
	Suriname	1	0	0
Europe		1166	624	78
	United Kingdom	518	293	41
	France	104	21	0
	Spain	97	92	5
	Germany	91	14	0
	Russia (south of 60º N)	85	71	18
	Bulgaria	60	6	0
	Italy	52	35	0
	Poland	40	25	1
	Portugal	33	17	0
	Ireland	32	17	1
	Austria	26	22	11
	Czech Republic	13	4	0

	Country	95th percentile (1000s of people)	50th percentile (1000s of people)	5th percentile (1000s of people)
	Albania	4	4	0
	Hungary	4	0	0
	Northern Cyprus	4	2	0
	Serbia	2	1	0
	Romania	0	0	0
Oceania		517	406	38
	Australia	504	400	37
	Papua New Guinea	8	4	0
	New Zealand	5	2	0
Africa		709	305	11
	Algeria	176	63	3
	South Africa	129	59	0
	Zambia	81	14	0
	Democratic Republic of the Congo	74	50	1
	Zimbabwe	37	24	5
	Rwanda	36	7	0
	Tanzania	35	21	1
	Burkina Faso	26	17	0
	Ghana	22	10	0
	Ethiopia	12	5	0
	Eritrea	10	4	0
	Sierra Leone	8	3	0
	Sudan	8	8	0
	Guinea	8	4	0
	Nigeria	7	2	0
	Niger	7	2	0
	Uganda	6	2	0
	Morocco	6	2	0
	Swaziland	5	3	0
	Kenya	5	2	0
	Gabon	5	0	0
	Liberia	3	2	0
	Mozambique	3	0	0

	Country	95th percentile (1000s of people)	50th percentile (1000s of people)	5th percentile (1000s of people)
	Angola	0	0	0
	Botswana	0	0	0
	Namibia	0	0	0
	Mauritania	0	0	0

Table S14: Impact of historical metal mining: Populations in floodplains contaminated by inactive mines. Areas of contaminated floodplains from inactive mines were estimated by the WAPHA model (95th, 50th and 5th percentile confidence intervals) and overlaid with GPWv4 gridded population to estimate population living in contaminated floodplains to the nearest 1000 people. Countries are listed by continent in descending order of populations affected with continental total rows shaded grey. Excludes territories with no floodplains mapped by GFPLAIN250.

	Status	**Percentile**	**N. America**	**S. America**	**Asia**	**Africa**	**Europe**	**Oceania**	**Total**
No. of mines	I		80,995	14,577	1,473	377	9,080	53,233	159,735
	A		11,871	3,240	1817	1,227	1024	3,430	22,609
River length affected (km)	I	5	49,370	11,540	3,000	600	1,160	33,340	99,010
		50	174,510	52,660	25,120	5,400	5,550	101,960	365,210
		95	208,570	68,710	42,110	9,260	8,120	119,430	456,200
	A	5	20,330	12,710	8,710	2,870	3,600	6,120	54,340
		50	23,880	29,060	35,780	11,920	9,240	4,130	114,000
		95	27,680	36,990	54,060	17,710	13,360	5,000	154,800
Floodplain area affected (km^2)	I	5	5,260	2,170	840	120	80	5,110	13,590
		50	36,710	23,800	14,650	3,150	1,570	32,510	112,390
		95	57,570	40,490	31,310	7,020	3,390	47,250	187,020
	A	5	3,910	2,770	2,490	660	640	1,380	11,840
		50	6,420	14,830	18,800	7,290	3,370	1,290	51,990
		95	9,110	23,560	34,000	13,330	6,970	1,860	88,820
100-year flood inundation area affected (km^2)	I	5	7,830	1,700	880	80	120	5,410	16,010
		50	58,870	18,320	15,540	2,350	1,900	40,340	137,320
		95	86,480	30,480	31,730	5,410	3,910	57,440	215,450
	A	5	3,990	2,360	2,640	540	740	1,630	11,890
		50	6,860	10,670	20,290	5,740	3,590	1,520	48,650
		95	8,860	16,260	36,300	10,830	6,710	2,240	81,200
Irrigated land in affected floodplain (km^2)	I	5	2,670	750	3010	0	50	1,430	5,200
		50	17,640	7,300	8,760	820	1,040	8,560	44,120
		95	26,610	11,550	17,960	1,700	2,070	12,910	72,810
	A	5	1,450	670	1,620	130	290	280	4,440
		50	2,120	4,900	11,090	1,130	1,920	310	21,450
		95	3,180	8,500	19,220	1,990	4,130	440	37,460
Population in affected floodplains (1000s)	I	5	467	113	538	11	78	38	1245
		50	3411	932	5716	305	624	406	11394
		95	5103	1571	11619	709	1166	517	20685
	A	5	475	193	2123	115	345	31	3282
		50	677	595	8811	883	1103	15	12084
		95	940	717	13681	1204	2083	15	18640
Livestock in affected floodplains (1000s)	I	5	70	50	20	0	0	310	450
		50	440	710	570	190	250	1,630	3,770
		95	840	1,120	1,330	320	330	2,020	5,970
	A	5	70	110	90	20	80	50	420
		50	120	440	810	360	140	70	1,950
		95	200	830	1,630	730	250	80	3,710

Table S15. Global assessment of hazard from metal mining contamination on river systems. As Table 1 in article but including confidence intervals. Number of inactive (I) and active (A) metal mines; river length, floodplain, 100-

year flood inundation and irrigated areas predicted to be affected by metal mining contamination with 90% confidence intervals; and number of livestock (cattle, goat and sheep) living on contaminated floodplains. With the exception of the number of mines, all figures are rounded to the nearest 10.

	Operating status	N. America	S. America	Asia	Africa	Europe	Oceania	Total
No. of mines	I	80,995	14,577	1,473	377	9,080	53,233	159,735
	A	11,871	3,240	1,817	1,227	1,024	3,430	22,609
River length affected (km)	I	174,510	52,660	25,120	5,400	5,550	101,960	365,210
	A	23,880	29,060	35,780	11,920	9,240	4,130	114,000
Floodplain area affected (km^2)	I	36,710	23,800	14,650	3,150	1,570	32,510	112,390
	A	6,420	14,830	18,800	7,290	3,370	1,290	51,990
100-year flood inundation area affected (km^2)	I	58,870	18,320	15,540	2,350	1,900	40,340	137,320
	A	6,860	10,670	20,290	5,740	3,590	1,520	48,650
Irrigated land in affected floodplain (km^2)	I	17,640	7,300	8,760	820	1,040	8,560	44,120
	A	2,120	4,900	11,090	1,130	1,920	310	21,450
Population in affected floodplains (1000s)	I	3,411	932	5,716	305	624	406	11,394
	A	677	595	8,811	883	1,103	15	12,084
Livestock in affected floodplains (1000s)	I	440	710	570	190	250	1,630	3,770
	A	120	440	810	360	140	70	1,950

Table S16. Global assessment of hazard from metal mining contamination on river systems. Number of inactive (I) and active (A) metal mines; river length, floodplain, 100-year flood inundation and irrigated areas predicted to be affected by metal mining contamination (see table S14 for confidence intervals); with human population and number of livestock (cattle, goat and sheep) living on contaminated floodplains. Except for the number of mines, all figures are rounded to the nearest 10.

	N. America	S. America	Asia	Africa	Europe	Oceania	Global
River length affected (km)	1,790	2,120	390	120	850	70	5,340
Floodplain area affected (km^2)	1,390	2,090	380	170	890	30	4,950
100-year flood inundation area affected (km^2)	1,130	1,540	340	110	660	20	3,800
Floodplain irrigated land affected (km^2)	30	1,190	200	130	110	0	1,660
Population in affected floodplains	9,970	195,870	93,370	8,260	15,170	150	322,790
Livestock in affected floodplains	9,820	87,110	22,530	6,610	6,570	0	132,640

Table S17. Global assessment of hazard from failed mine tailings storage facilities. Modelled contamination from 165 failed tailings storage facilities (TSF) for which runout distances were observed from the total of 257 failed TSF recorded in the WAPHA database. Predictions of contamination were derived from the WAPHA model using the observed runout distances. All figures are rounded to the nearest 10.

Reference List

1. PWC, "Mine 2018: Tempting Times", (2018) https://www.pwc.com/id/en/publications/assets/eumpublications/mining/mine-2018.pdf.
2. U. Förstner, "Introduction" in *Environmental Impacts of Mining Activities: Emphasis on Mitigation and Remedial Measures,* J. M. Azcue, Ed. (Springer, 1999), pp. 1-3.
3. J. Syvitski *et al.*, Earth's sediment cycle during the Anthropocene. *Nature Reviews Earth and Environment* **3**, 179-196 (2022).
4. B. G. Lottermoser, *Mine Wastes: Characterization, Treatment and Environmental Impacts* (Springer, ed. 3, 2010).
5. K. A. Hudson-Edwards, Tackling mine wastes. *Science* **352**, 288-290 (2016).
6. J. E. Gall *et al.*, Transfer of heavy metals through terrestrial food webs: a review. *Environ Monit Assess* **187**, 201 (2015).
7. J. R. Miller *et al.*, Heavy metal contamination of water, soil and produce within riverine communities of the Rio Pilcomayo basin, Bolivia. *Sci Total Environ* **320**, 189-209 (2004).
8. D. Xu *et al.*, Effects of soil properties on heavy metal bioavailability and accumulation in crop grains under different farmland use patterns. *Sci Rep-Uk* **12**, 9211 (2022).
9. M. Roy, L. M. McDonald, Metal Uptake in Plants and Health Risk Assessments in Metal-Contaminated Smelter Soils. *Land Degradation & Development* **26**, 785-792 (2015).
10. S. A. Foulds *et al.*, Flood-related contamination in catchments affected by historical metal mining: An unexpected and emerging hazard of climate change. *Sci Total Environ* **476**, 165-180 (2014).
11. S. Giri, A. K. Singh, Human health risk assessment due to metals in cow's milk from Singhbhum copper and iron mining areas, India. *J Food Sci Technol* **57**, 1415-1420 (2020).
12. H. Ali, E. Khan, Bioaccumulation of non-essential hazardous heavy metals and metalloids in freshwater fish. Risk to human health. *Environmental Chemistry Letters* **16**, 903-917 (2018).
13. Y. Jia *et al.*, Distribution, contamination and accumulation of heavy metals in water, sediments, and freshwater shellfish from Liuyang River, Southern China. *Environ Sci Pollut R* **25**, 7012-7020 (2018).
14. S. Mwelwa *et al.*, Biotransfer of heavy metals along the soil-plant-edible insect-human food chain in Africa. *Sci Total Environ* **881**, 163150 (2023).
15. J. P. Grattan *et al.*, The first polluted river? Repeated copper contamination of fluvial sediments associated with Late Neolithic human activity in southern Jordan. *Sci Total Environ* **573**, 247-257 (2016).
16. D. Kossoff *et al.*, Mine tailings dams: Characteristics, failure, environmental impacts, and remediation. *Appl Geochem* **51**, 229-245 (2014).
17. J. Lewin *et al.*, "Interactions Between Channel Change and Historic Mining Sediments" in *River Channel Changes*, K. J. Gregory, Ed. (John Wiley and Sons, 1977), pp. 353-367.
18. J. Lewin, M. G. Macklin, "Metal mining and floodplain sedimentation in Britain" in *International Geomorphology Part 1,* V. Gardiner, Ed. (John Wiley and Sons, 1987), pp. 1009-1027.
19. W. L. Graf *et al.*, Geomorphology of Heavy-Metals in the Sediments of Queen-Creek, Arizona, USA. *Catena* **18**, 567-582 (1991).

20. M. G. Macklin, J. Lewin, Sediment Transfer and Transformation of an Alluvial Valley Floor - the River South Tyne, Northumbria, UK. *Earth Surf Proc Land* **14**, 233-246 (1989).
21. M. G. Macklin, R. B. Dowsett, The Chemical and Physical Speciation of Trace-Metals in Fine-Grained Overbank Flood Sediments in the Tyne Basin, Northeast England. *Catena* **16**, 135-151 (1989).
22. M. G. Macklin *et al.*, The significance of pollution from historic metal mining in the Pennine orefields on river sediment contaminant fluxes to the North Sea. *Sci Total Environ* **194**, 391-397 (1997).
23. J. M. Martin, M. Meybeck, Elemental Mass-Balance of Material Carried by Major World Rivers. *Mar Chem* **7**, 173-206 (1979).
24. I. A. Dennis *et al.*, The impact of the October-November 2000 floods on contaminant metal dispersal in the River Swale catchment, North Yorkshire, UK. *Hydrol Process* **17**, 1641-1657 (2003).
25. M. G. Macklin *et al.*, A geomorphological approach to the management of rivers contaminated by metal mining. *Geomorphology* **79**, 423-447 (2006).
26. I. A. Dennis *et al.*, The role of floodplains in attenuating contaminated sediment fluxes in formerly mined drainage basins. *Earth Surf Proc Land* **34**, 453-466 (2009).
27. D. Ciszewski, T. M. Grygar, A Review of Flood-Related Storage and Remobilization of Heavy Metal Pollutants in River Systems. *Water Air Soil Poll* **227**, (2016).
28. M. G. Macklin *et al.*, Materials and Methods for: Impacts of metal mining on river systems: a global assessment. (Supplementary Information, 2023).
29. "Water and Planetary Health Analytics (WAPHA) Global Metal Mines Database", (2023);
30. QGIS Association, "QGIS Geographic Information System", (2023); http://www.qgis.org/.
31. USGS, "Mineral Resources Data System (MRDS)", (2022); https://mrdata.usgs.gov/mrds/.
32. BGS, "User Guide: BGS BritPIts", (2021); https://www.bgs.ac.uk/datasets/britpits/.
33. S&P Global Market Intelligence, "S&P Capital IQ Pro platform", https://www.spglobal.com/marketintelligence/en/campaigns/metals-mining.
34. ICOLD, *Tailings Dams: Risk of Dangerous Occurrences : Lessons Learnt from Practical Experiences (bulletin 121)*. (Commission Internationale des Grand Barrages, 2001).
35. WISE Uranium Project, "Chronology of major tailings dam failures (1960-2022)", (2022); https://wise-uranium.org/mdaf.html.
36. GTP, "Global Tailings Portal", https://tailing.grida.no/.
37. "MATLAB version: 9.9.0 (R2020b), Natick, Massachusetts: The MathWorks Inc", (2020); https://www.mathworks.com.
38. HydroSheds, "Seamless hydrographic data for global and regional applications v1", https://www.hydrosheds.org/.
39. P. Concha Larrauri, U. Lall, Tailings Dams Failures: Updated Statistical Model for Discharge Volume and Runout. *Environments* **5**, (2018).
40. NASA, "Gridded Population of the World (GPW), v4 rev 10", (2016); https://sedac.ciesin.columbia.edu/data/collection/gpw-v4/whatsnewrev10.
41. FAO, "Gridded Livestock of the World (GLW3)", (2010); https://www.fao.org/land-water/land/land-governance/land-resources-planning-toolbox/category/details/fr/c/1236449/.

42. G. Bird *et al.*, Dispersal of Contaminant Metals in the Mining-Affected Danube and Maritsa Drainage Basins, Bulgaria, Eastern Europe. *Water Air Soil Poll* **206**, 105-127 (2010).
43. P. E. a. G. C. Switzerland, "World's Worst Pollution Problems: The Toxins Beneath Our Feet", (2016) http://www.worstpolluted.org/2016-report.html.
44. K. B. Ding *et al.*, Ecosystem services provided by heavy metal-contaminated soils in China. *J Soil Sediment* **18**, 380-390 (2018).
45. C. Baker-Austin *et al.*, Co-selection of antibiotic and metal resistance. *Trends in Microbiology* **14**, 176-182 (2006).
46. P. Kinnunen *et al.*, Local food crop production can fulfil demand for less than one-third of the population. *Nature Food* **1**, 229-237 (2020).
47. R. Gandolff, Lead exposure in childhood and historical land use: a geostatistical analysis of soil lead concentrations in South Philadelphia parks. *Environ Monit Assess* **195**, 356 (2023).
48. D. Huerta *et al.*, Probabilistic risk assessment of residential exposure to metal(loid)s in a mining impacted community. *Sci Total Environ* **872**, 162228 (2023).
49. M. A. Oliver, P. J. Gregory, Soil, food security and human health: a review. *European Journal of Soil Science* **66**, 257-276 (2015).
50. L. A. Naylor *et al.*, Stormy geomorphology: geomorphic contributions in an age of climate extremes. *Earth Surf Proc Land* **42**, 166-190 (2017).
51. A. Weber *et al.*, The risk may not be limited to flooding: polluted flood sediments pose a human health threat to the unaware public. *Environmental Sciences Europe* **35**, 58 (2023).
52. B. Tellman *et al.*, Satellite imaging reveals increased proportion of population exposed to floods. *Nature* **596**, 80-86 (2021).
53. J. R. Owen *et al.*, Catastrophic tailings dam failures and disaster risk disclosure. *International Journal of Disaster Risk Reduction* **42**, 101361 (2020).
54. L. Tang, T. T. Werner, Global mining footprint mapped from high-resolution satellite imagery. *Communications Earth & Environment* **4**, 134 (2023).
55. ICOLD, *Tailings Dams: Risk of Dangerous Occurrences : Lessons Learnt from Practical Experiences*. (Commission Internationale des Grand Barrages, 2001).
56. J. Liu *et al.*, A Bayesian Network-based risk dynamic simulation model for accidental water pollution discharge of mine tailings ponds at watershed-scale. *J Environ Manage* **246**, 821-831 (2019).
57. G. Z. Yin *et al.*, Stability analysis of a copper tailings dam via laboratory model tests: A Chinese case study. *Miner Eng* **24**, 122-130 (2011).
58. E. Lebre *et al.*, Source Risks As Constraints to Future Metal Supply. *Environ Sci Technol* **53**, 10571-10579 (2019).
59. E. Lebre *et al.*, The social and environmental complexities of extracting energy transition metals. *Nat Commun* **11**, (2020).
60. L. J. Sonter *et al.*, Renewable energy production will exacerbate mining threats to biodiversity. *Nat Commun* **11**, (2020).
61. D. M. Franks *et al.*, Tailings facility disclosures reveal stability risks. *Sci Rep-Uk* **11**, (2021).
62. J. Lewin, M. G. Macklin, "Metal mining and floodplain sedimentation in Britain." in *International Geomorphology Part 1,* V. Gardiner, Ed. (Wiley, 1986), pp. 1009-1027.

63. G. Bird *et al.*, Pb isotope evidence for contaminant-metal dispersal in an international river system: The lower Danube catchment, Eastern Europe. *Appl Geochem* **25**, 1070-1084 (2010).
64. G. Bird *et al.*, The solid state partitioning of contaminant metals and As in river channel sediments of the mining affected Tisa drainage basin, northwestern Romania and eastern Hungary. *Appl Geochem* **18**, 1583-1595 (2003).
65. G. Bird *et al.*, Heavy metal contamination in the Aries river catchment, western Romania: Implications for development of the Rosia Montand gold deposit. *J Geochem Explor* **86**, 26-48 (2005).
66. K. A. Hudson-Edwards *et al.*, The impact of tailings dam spills and clean-up operations on sediment and water quality in river systems: the Rios Agrio-Guadiamar, Aznalcollar, Spain. *Appl Geochem* **18**, 221-239 (2003).
67. M. P. Taylor, K. A. Hudson-Edwards, The dispersal and storage of sediment-associated metals in an and river system: The Leichhardt River, Mount Isa, Queensland, Australia. *Environ Pollut* **152**, 193-204 (2008).
68. G. Bird *et al.*, River system recovery following the Novat-Rosu tailings dam failure, Maramures County, Romania. *Appl Geochem* **23**, 3498-3518 (2008).
69. G. Bird *et al.*, The impact and significance of metal mining activities on the environmental quality of Romanian river systems. (2003), pp. 316-322.
70. G. Bird *et al.*, Quantifying sediment-associated metal dispersal using Pb isotopes: Application of binary and multivariate mixing models at the catchment-scale. *Environ Pollut* **158**, 2158-2169 (2010).
71. P. Byrne *et al.*, Water quality impacts and river system recovery following the 2014 Mount Polley mine tailings dam spill, British Columbia, Canada. *Appl Geochem* **91**, 64-74 (2018).
72. D. Ciszewski, Source of pollution as a factor controlling distribution of heavy metals in bottom sediments of Chechlo River (south Poland). *Environ Geol* **29**, 50-57 (1997).
73. K. A. Hudson-Edwards *et al.*, Sources, distribution and storage of heavy metals in the Rio Pilcomayo, Bolivia. *J Geochem Explor* **72**, 229-250 (2001).
74. A. R. Karbassi *et al.*, Metal pollution assessment of sediment and water in the Shur River. *Environ Monit Assess* **147**, 107-116 (2008).
75. M. G. Macklin, “Fluxes and storage of sediment-associated heavy metals in floodplain systems: assessment and river basin management issue as at a time of rapid environmental change.” in *Floodplain processes*, M. G. Anderson, D. E. Walling, P. D. Bates, Eds. (Wiley, 1996), pp. 441-460.
76. M. G. Macklin *et al.*, “Review of the Porco Mine Tailings Dam Burst and Associated Mining Waste Problems, Pilcomayo Basin, Bolivia.”, (1996)
77. W. M. Mayes *et al.*, Dispersal and Attenuation of Trace Contaminants Downstream of the Ajka Bauxite Residue (Red Mud) Depository Failure, Hungary. *Environ Sci Technol* **45**, 5147-5155 (2011).
78. J. N. Turner *et al.*, Heavy metals and As transport under low and high flows in the River Guadiamar three years after the Aznalcóllar tailings dam failure : implications for river recovery and management. *Cuad. Investig. Geográfica 28, 31 (2002).* **28**, 31-47 (2002).
79. V. Ettler *et al.*, Geochemical and Pb isotopic evidence for sources and dispersal of metal contamination in stream sediments from the mining and smelting district of Pribram, Czech Republic. *Environ Pollut* **142**, 409-417 (2006).

80. M. Gutierrez *et al.*, Mobility of Metals in Sediments Contaminated with Historical Mining Wastes: Example from the Tri-State Mining District, USA. *Soil Syst* **3**, (2019).
81. ICPDR, "Analysis of the Tisza River Basin 2007. Initial step toward the Tisza River Basin Management Plan", (2009) https://www.icpdr.org/main/sites/default/files/Tisza_RB_Analysis_2007.pdf.
82. C. G. Lee *et al.*, Heavy metal contamination in the vicinity of the Daduk Au-Ag-Pb-Zn mine in Korea. *Appl Geochem* **16**, 1377-1386 (2001).
83. J. S. Lee, H. T. Chon, Hydrogeochemical characteristics of acid mine drainage in the vicinity of an abandoned mine, Daduk Creek, Korea. *J Geochem Explor* **88**, 37-40 (2006).
84. M. G. Macklin *et al.*, The long term fate and environmental significance of contaminant metals released by the January and March 2000 mining tailings dam failures in Maramures County, upper Tisa Basin, Romania. *Appl Geochem* **18**, 241-257 (2003).
85. R. T. Pavlowsky *et al.*, Legacy sediment, lead, and zinc storage in channel and floodplain deposits of the Big River, Old Lead Belt Mining District, Missouri, USA. *Geomorphology* **299**, 54-75 (2017).
86. P. Renforth *et al.*, Contaminant mobility and carbon sequestration downstream of the Ajka (Hungary) red mud spill: The effects of gypsum dosing. *Sci Total Environ* **421**, 253-259 (2012).
87. J. N. Turner *et al.*, Fluvial-controlled metal and As mobilisation, dispersal and storage in the Rio Guadiamar, SW Spain and its implications for long-term contaminant fluxes to the Donana wetlands. *Sci Total Environ* **394**, 144-161 (2008).
88. W. J. F. Visser, "Contaminated Land Policies in Some Industrialised Countries ", (The Hague, 2500 GX, The Netherlands 1993) http://www.eugris.info/newsdownloads/WilmaVisserReport.pdf.
89. W. J. F. Visser, Contaminated Land Policies in Europe. *Chem Ind-London*, 496-499 (1995).
90. D. Yamazaki *et al.*, A high-accuracy map of global terrain elevations. *Geophys Res Lett* **44**, 5844-5853 (2017).
91. F. Nardi *et al.*, GFPLAIN250m, a global high-resolution dataset of Earth's floodplains. *Sci Data* **6**, (2019).
92. P. Scussolini *et al.*, Global River Discharge and Floods in the Warmer Climate of the Last Interglacial. *Geophys Res Lett* **47**, 1-12 (2020).
93. S. Siebert *et al.*, "Update of the Digital Global Map of Irrigation Areas to Version 5", (2013) https://www.fao.org/3/I9261EN/i9261en.pdf.
94. W. Schwanghart, D. Scherler, Short Communication: TopoToolbox 2-MATLAB-based software for topographic analysis and modeling in Earth surface sciences. *Earth Surf Dynam* **2**, 1-7 (2014).
95. H. Leenaers, *The dispersal of metal mining wastes in the catchment of the river Geul (Belgium - The Netherlands)*. (Utrecht, 1989), pp. 230.
96. P. A. Brewer *et al.*, "The use of geomorphological mapping and modelling for identifying land affected by metal contamination on river floodplains. ", (2003)
97. K. A. Hudson-Edwards *et al.*, "Assessment of metal mining-contaminated river sediments in England and Wales", (Environment Agency,2008)
98. ESDAT, "Circular on target values and intervention values for soil remediation.", www.esdat.net.

99. P. Ashton *et al.*, "An overview of the impact of mining and mineral processing operations on water resources and water quality in the Zambezi, Limpopo and Olifants catchments in southern Africa", (CSIREnvironmentek, Pretoria, South Africa and Geology Department, University of Zimbabwe, Harare, Zimbabwe,2001) https://iied.org/sites/default/files/pdfs/migrate/G02404.pdf.
100. M. C. W. Lourens, T, D., "Operating Mines and Quarries and Mineral Processing 203 Plants in the Republic of South Africa (Directory D1/2016). ", (2016) https://www.resourcedata.org/dataset/rgi-operating-mines-and-quarries-and-mineral-processing-plants-in-the-republic-of-south-africa-2016.
101. P. Chuhan-Pole *et al.*, *Mining in Africa: Are Local Communities Better Off?* , Mining in Africa: Are Local Communities Better Off? (The World Bank, 2017).
102. Deloitte, "Industry Outlook Mining in Argentina.", (2016) https://www2.deloitte.com/content/dam/Deloitte/ar/Documents/finance/Industry%20Outlook%20-%20Mining%20in%20Argentina.pdf.
103. Australian Government, "Australian Mines Atlas", https://portal.ga.gov.au/persona/minesatlas.
104. T. T. Werner *et al.*, A Geospatial Database for Effective Mine Rehabilitation in Australia. *Minerals-Basel* **10**, (2020).
105. "Government of The Wallonia - Brussels Federation", https://www.arcgis.com/home/webmap/viewer.html?featurecollection=https%3A%2F%2Fgeoservices.wallonie.be%2Farcgis%2Frest%2Fservices%2FSOL_SOUS_SOL%3Ff%3Djson%26option%3Dfootprints&supportsProjection=true&supportsJSONP=true.
106. L. J. Sonter *et al.*, Renewable energy production will exacerbate mining threats to biodiversity. *Nat Commun* **11**, 1-6 (2020).
107. Hudson Institute of Mineralogy, "Mines, Minerals and More", https://www.mindat.org/.
108. "National Mining Dams Registry", http://www.anm.gov.br/assuntos/barragens/pasta-cadastro-nacional-de-barragens-de-mineracao/cadastro-nacional-de-barragens-de-mineracao .
109. SeeNews, "Gold Mining and Processing in Bulgaria", (2010); https://seenews.com/reports/industry_report/gold-mining-and-processing-bulgaria-2010-58.
110. Government of Canada, "Principal mineral areas, producing mines, and oil and gas fields in Canada / Lands and Minerals Sector and National Energy Board ", (2021); https://publications.gc.ca/site/eng/9.853130/publication.html.
111. Media Edge Publishing, "Ontario Mining & Exploration Directory - 2021", (2021); https://www.mndm.gov.on.ca/en/news/mines-and-minerals/ontario-mining-exploration-directory-2021.
112. B. G. Wei, L. S. Yang, A review of heavy metal contaminations in urban soils, urban road dusts and agricultural soils from China. *Microchem J* **94**, 99-107 (2010).
113. Z. Y. Li *et al.*, A review of soil heavy metal pollution from mines in China: Pollution and health risk assessment. *Sci Total Environ* **468**, 843-853 (2014).
114. H. Y. Chen *et al.*, Contamination features and health risk of soil heavy metals in China. *Sci Total Environ* **512**, 143-153 (2015).
115. X. M. Chen *et al.*, Speciation and distribution of mercury in soils around gold mines located upstream of Miyun Reservoir, Beijing, China. *J Geochem Explor* **163**, 1-9 (2016).
116. X. W. Zhang *et al.*, Impacts of lead/zinc mining and smelting on the environment and human health in China. *Environ Monit Assess* **184**, 2261-2273 (2012).

117. J. Pinedo-Hernandez *et al.*, Speciation and bioavailability of mercury in sediments impacted by gold mining in Colombia. *Chemosphere* **119**, 1289-1295 (2015).
118. "Cuba Economic Activity Map 1977", https://www.gifex.com/cuba_maps/Cuba_Economic_Activity_Map_2.htm.
119. V. Štrupl *et al.*, Current state of registered hazardous abandoned mine waste facilities in the Czech Republic. *Geoscience Research Reports* **50**, 95-97 (2017).
120. M. L. Räisänen *et al.*, "Suljettujen ja hylättyjen kaivosten kaivannaisjätealueiden kartoitus. (Mapping of mine waste areas in closed and abandoned mines)", (2013) https://helda.helsinki.fi/bitstream/handle/10138/41486/YMra_24_2013.pdf?sequence=1&isAllowed=y.
121. K. Nasri *et al.*, Unlikely lead-bearing phases in river and estuary sediments near an ancient mine (Huelgoat, Brittany, France). *Environ Sci Pollut R* **28**, 8128-8139 (2021).
122. Federal Institute for Geosciences and Natural Resources, "Map of Mining and Storage Operations of the Federal Republic of Germany 1 : 2 000 000 (BergSP)", https://www.bgr.bund.de/EN/Themen/Sammlungen-Grundlagen/GG_geol_Info/Karten/Deutschland/Kt_Bergbau/bergSP_inhalt_en.html?nn=1556480.
123. Mining and Geological Survey of Hungary, "Mining areas in Hungary", (2022); https://mbfsz.gov.hu/en/node/408.
124. Ministry of Mines. Government of India, "Mineral Map of India", https://www.mines.gov.in/UserView/index?mid=1272.
125. EPA Ireland, "EPA GeoPortal - Historic Mines project", https://gis.epa.ie/GetData/Download.
126. Istituto Superiore per la Protezione e la Ricerca Ambientale, "Database cave e miniere servizio geologico d'Italia - GEMMA", https://www.isprambiente.gov.it/it/progetti/cartella-progetti-in-corso/suolo-e-territorio-1/miniere-e-cave/progetto-remi-rete-nazionale-dei-parchi-e-musei-minerari-italiani/banche-dati/database-nazionale-cave-miniere-servizio-geologico-d2019italia.
127. V. Bogdetsky, V. Novikov, "Mining, development and environment in Central Asia: Toolkit Companion with case studies", (2012) https://wedocs.unep.org/handle/20.500.11822/7549.
128. Central Asian Geoportal, "Geological and mineral resources map ", https://cac-geoportal.org/.
129. P. Kyophilavong, "Mining Sector in Laos" in *BRC Discussion Paper Series No. 18, Edition 1*, I.-J. Bangkok Research Center (BRC), Ed. (Bangkok Research Center (BRC), 2009), pp. 69-100.
130. University of Texas, "Mexico Mining and Industry", https://maps.lib.utexas.edu/maps/americas/mexico_industry_1978.jpg.
131. Geo-Mexico, "The geography of gold mining in Mexico", (2013); https://geo-mexico.com/?p=9658.
132. N. J. Gardiner *et al.*, The metallogenic provinces of Myanmar. *Applied Earth Science* **123**, 25-38 (2014).
133. N. J. Gardiner *et al.*, Tin mining in Myanmar: Production and potential. *Resour Policy* **46**, 219-233 (2015).
134. E. B. Eckel *et al.*, "Geology and mineral resources of Paraguay--a reconnaissance, with sections on Igneous and metamorphic rocks and soils", *Professional Paper* (1959) http://pubs.er.usgs.gov/publication/pp327.

135. PWC, "Doing Business in Peru - Mining Chapter", (2020) https://www.pwc.pe/es/publicaciones/assets/PwC-Doing-Business-in-Peru-Mining.pdf.

136. A. van Geen *et al.*, Lead exposure from soil in Peruvian mining towns: a national assessment supported by two contrasting. examples. *B World Health Organ* **90**, 878-886 (2012).

137. LNEG, "Portugal - Exploration and Mining", (2000) https://geoportal.lneg.pt/pt/bds/siorminp#!/.

138. European Commission, "Extractive Waste - Closed and abandoned waste facilities (2017).", (2017); https://www.economie.gov.ro/images/legislatie/Resurse%20Minerale/Inventar_Iazuri_de_Decantare_iulie_2012.pdf.

139. T. R. Walker *et al.*, Anthropogenic metal enrichment of snow and soil in north-eastern European Russia. *Environ Pollut* **121**, 11-21 (2003).

140. J. Jarsjo *et al.*, Patterns of soil contamination, erosion and river loading of metals in a gold mining region of northern Mongolia. *Reg Environ Change* **17**, 1991-2005 (2017).

141. J. Monthel *et al.*, "Mineral deposits and mining districts of Serbia - Compilation map and GIS databases", (2002) http://gras.org.rs/wp-content/uploads/2017/10/mineral-deposits-and-mining-districts-of-serbia.pdf.

142. N. Atanackovic *et al.*, Regional-scale screening of groundwater pollution risk induced by historical mining activities in Serbia. *Environ Earth Sci* **75**, (2016).

143. Slovak Environment Agency "Information system on extractive waste management", https://app.sazp.sk/Odpady_tp/About.aspx.

144. M. Gosar *et al.*, "Preparation of a list of enclosed facilities for the management of waste from mining and other mineral resource mining activities : report of the 3rd phase of the project. (Geological Survey of Slovenia, 2014).", (2014)

145. T. Assawincharoenkij *et al.*, Mineralogical and geochemical characterization of waste rocks from a gold mine in northeastern Thailand: application for environmental impact protection. *Environ Sci Pollut R* **25**, 3488-3500 (2018).

146. X. Li *et al.*, Recent evolution of the Mekong Delta and the impacts of dams. *Earth-Sci Rev* **175**, 1-17 (2017).

147. D. Potter, D. Johnston, "Inventory of closed mining waste facilities", (Environment Agency,2014) https://assets.publishing.service.gov.uk/government/uploads/system/uploads/attachment_data/file/288582/LIT_6797_7d390c.pdf.

148. F. Santos-Frances *et al.*, Distribution and mobility of mercury in soils of a gold mining region, Cuyuni river basin, Venezuela. *J Environ Manage* **92**, 1268-1276 (2011).

149. P. G. Schruben *et al.*, "Geology and mineral resource assessment of the Venezuelan Guayana Shield at 1:500,000 scale; a digital representation of maps published by the U.S. Geological Survey", (USGS,1997) https://pubs.usgs.gov/dds/dds46/.

150. M. M. B. Veiga, D. *et al.*, "Mercury Pollution from Artisanal Gold Mining" in *Dynamics of Mercury Pollution on Regional and Global Scales*, N. Pirrone, K. R. Mahaffey, Eds. (Springer, Boston, MA, 2005), pp. 421-450.

151. United States Government, "U. S. Government open data portal", https://catalog.data.gov/dataset?tags=mines.

152. L. N. Bowker, D. M. Chambers, "The Risk, Public Liability, and Economics of Tailings Storage Facility Failures. 2015. ", (2015) http://www.csp2.org/files/reports/Bowker%20%26%20Chambers%20-%20Risk-

Public%20Liability-Economics%20of%20Tailings%20Storage%20Facility%20Failures%20%E2%80%93%2023Jul15.pdf.

153. Q. T. Li *et al.*, Detection of Tailings Dams Using High-Resolution Satellite Imagery and a Single Shot Multibox Detector in the Jing-Jin-Ji Region, China. *Remote Sens-Basel* **12**, (2020).

154. L. Tang *et al.*, Statistical analysis of tailings ponds in China. *J Geochem Explor* **216**, (2020).